Available online at www.sciencedirect.com
ScienceDirect
Polymer 48 (2007) 6181–6204
polymer
www.elsevier.com/locate/polymer

Feature Article

Acetylenes with multiple triple bonds: A group of versatile A_n-type building blocks for the construction of functional hyperbranched polymers

Matthias Häußler [a], Anjun Qin [a,b], Ben Zhong Tang [a,b,*]

[a] Department of Chemistry, The Hong Kong University of Science & Technology, Clear Water Bay, Kowloon, Hong Kong, China
[b] Department of Polymer Science and Engineering, Zhejiang University, Hangzhou 310027, China

Received 2 July 2007; received in revised form 6 August 2007; accepted 10 August 2007
Available online 22 August 2007

Abstract

AB_n-type monomers have been widely used for the synthesis of hyperbranched polymers. These monomers, however, suffer from the problems associated with the tendency of their mutually reactive A and B functional groups toward self-oligomerization. We have explored the possibility of synthesizing hyperbranched polymers using A_n-type monomers, which are stable and easy to prepare and handle, with some being even commercially available. In particular, we have tried to open new synthetic routes to hyperbranched polymers using diynes and triynes as monomers. We have developed metallic [$TaBr_5$, $Cp^*Ru(PPh_3)_2Cl$, etc.] and nonmetallic catalysts (piperidine, DMF, etc.) for polycyclotrimerization, polycycloaddition and polycoupling of the acetylenic monomers. We have synthesized a variety of new hyperbranched polymers including polyarylenes, polytriazoles and polydiynes with high molecular weights and excellent solubility in high yields. The polymers exhibit an array of functional properties such as sensitive photonic response, high light refractivity, large optical nonlinearity, high thermal stability, strong optical limiting power and unusual aggregation-enhanced light emission. Utilizing these unique properties, we succeeded in generating fluorescent images, honeycomb patterns, polymer nanotubes, ferromagnetic ceramics, and nanoparticle catalysts.

Keywords: Acetylene polymerization; Hyperbranched polymers; Functional materials

1. Introduction

Most commodity plastics used in the contemporary society such as polypropylene (PP), polystyrene (PS) and poly(methyl methacrylate) (PMMA) are manufactured by the chain polymerizations of vinyl monomers. In other words, conventional chain polymerization is mainly based on olefin chemistry. When vinyl monomers are polymerized, their double bonds are transformed into single bonds, giving saturated polymers with electrical and optical inactivities. Whereas an enormous amount of research has been done on olefin polymerization, acetylene chemistry has been much less utilized in the polymer synthesis, in spite of the promise that acetylene polymerizations can generate unsaturated or conjugated polymers with electrical conductivity, optical activity, and photonic susceptibility [1–3].

A dozen of research groups in the world have done some pioneering work in the area of acetylene polymerizations [4–15]. The area is, however, still full of challenges. For example, most catalysts for acetylene polymerizations are labile transition-metal salts or sensitive organometallic complexes; their stable organic congeners or organocatalysts are virtually unknown. Only a few types of acetylene reactions have been successfully developed into useful polymerization techniques, and it has been difficult to polymerize functionalized acetylene monomers because many of the traditional catalysts have little tolerance to polar groups. Many acetylene-based conjugated polymers are unstable, which has greatly limited the scope of their practical applications. Almost all acetylene polymers

* Corresponding author. Department of Chemistry, The Hong Kong University of Science & Technology, Clear Water Bay, Kowloon, Hong Kong, China. Tel.: +852 2358 7375; fax: +852 2358 1594.
E-mail address: tangbenz@ust.hk (B.Z. Tang).

0032-3861/$ - see front matter © 2007 Elsevier Ltd. All rights reserved.
doi:10.1016/j.polymer.2007.08.044

with high molecular weights possess a linear structure, and few hyperbranched polymers have been derived from acetylene monomers.

Attracted by the great variety of acetylene derivatives and their fabulously rich reactivities [15–17], we have embarked upon a research program on acetylene polymerizations, with the aim of developing new polymerization techniques based on acetylene chemistry and cultivating acetylenic compounds into versatile building blocks for the construction of new conjugated macromolecules. We have previously focused our attention on the syntheses of linear polyacetylenes from acetylene monomers with single triple bonds or monoynes (Scheme 1). Our effort in the exploration of functionality-tolerant catalysts and the optimization of polymerization processes has enabled us to successfully prepare a large number of functional polyacetylenes with various pendant groups. In addition to being stable and processable, the new polyacetylenes with appropriate skeleton–pendant combinations have shown an array of novel properties, such as luminescence, photoconductivity, photonic patternability, helical chirality, liquid crystallinity, optical nonlinearity, solvatochromism, cytocompatibility, and biological activity [18,19]. The properties of the polyacetylenes can be tuned internally and manipulated externally: the former is accomplished by varying their molecular structures, especially their functional pendants, while the latter is achieved by applying thermal, mechanical, electrical, photonic, and chemical stimuli [18].

We have recently extended our research effort from one-dimensional to three-dimensional systems and have worked on the syntheses of nonlinear hyperbranched polymers from acetylenic monomers having two and three triple bonds or diynes and triynes (Scheme 2). In this Feature Article, we will briefly review our work in this area of research: we will summarize our results on the polymer syntheses, outline the functional properties of the new polymers, and illustrate their potential applications. We have successfully developed new catalysts for acetylene polymerizations, especially the organocatalysts with great functionality-tolerance. We have established new synthetic routes to hyperbranched polymers and prepared new polyphenylenes, polydiynes and polytriazoles by polycyclotrimerization, polycoupling and polycycloaddition reactions of diyne and triyne monomers. Traditionally, hyperbranched polymers have often been prepared from polycondensations of AB_n ($n \geq 2$), especially AB_2, monomers (Scheme 3). The new A_n ($n = 2, 3$) protocol developed in this study provides polymer chemists with a new synthetic tool that is free of the complications suffered by the AB_2 system, such as the difficulty in the monomer preparation, isolation and storage, because of the coexistence of two mutually reactive groups A and B in one monomer species [20–26]. The new

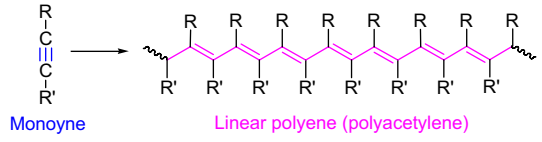

Scheme 1. Synthesis of linear polyacetylenes from monoyne monomers.

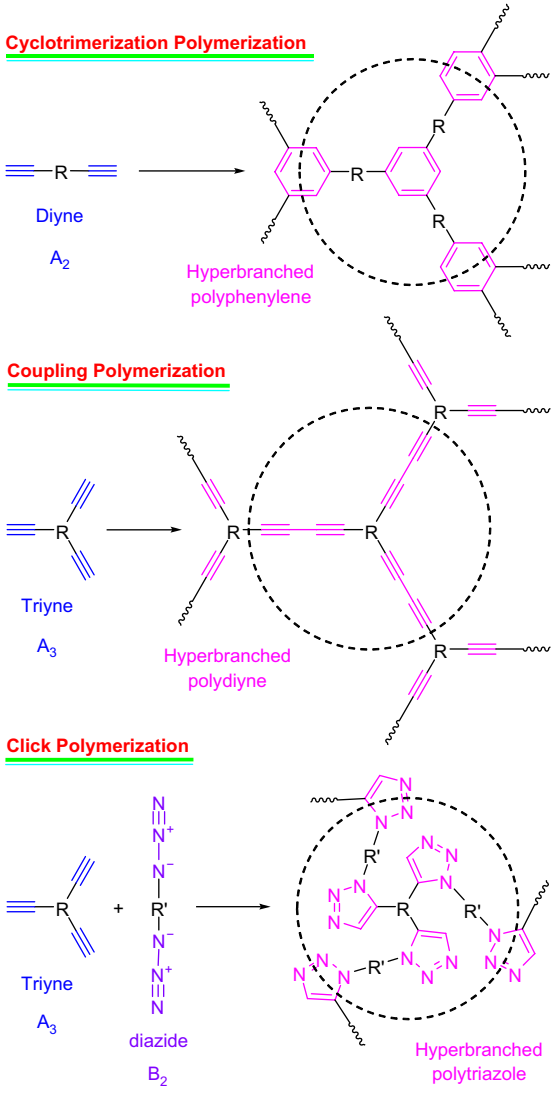

Scheme 2. Syntheses of nonlinear hyperbranched polyphenylenes, polydiynes and polytriazoles by polycyclotrimerization, polycoupling and polycycloaddition of diyne, triyne and diazide monomers.

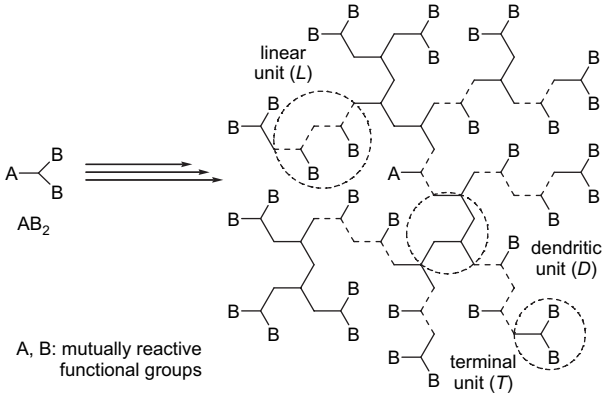

Scheme 3. A common approach to hyperbranched polymers with structural illustration of the dendritic, linear and terminal units.

hyperbranched polymers have been found to show unique properties including thermal curability, photonic susceptibility, pattern formation, fluorescent imaging, light refraction, optical nonlinearity, and metallic complexation. Furthermore, the metallized polymers can be readily pyrolyzed into soft ferromagnetic ceramics with high magnetizability and into nanoparticles with catalytic activity for carbon nanotube fabrication.

2. Hyperbranched poly(alkylenephenylenes) (hb-PAPs)

Acetylene cyclotrimerization is a century-old reaction for the effective transformation of monoyne molecules to benzene rings. When this reaction is applied to diyne molecules, hyperbranched polymers may be generated. This A_2 polycyclotrimerization approach will circumvent the synthetic difficulties encountered by the AB_2 system and produce stable polymers consisting of robust benzene rings. With these anticipations in mind, we started our work on the synthesis of hyperbranched polymers by diyne polycyclotrimerization.

2.1. Synthesis

We first studied the homopolycyclotrimerizations of aliphatic diynes with different lengths of alkyl spacers (Scheme 4) [27–31]. Binary mixtures of MtX_5 and Ph_4Sn were found to be effective catalysts for polycyclotrimerizations of terminal and internal diyne monomers. We investigated the effects of parameters such as monomer structure, reaction time, monomer/catalyst concentration, etc. on the diyne polycyclotrimerization. A ''right'' combination of these factors ensured the polymerization reactions to proceed smoothly. Under optimal conditions, completely soluble homopolymers with high molecular weights (M_w up to $\sim 1.4 \times 10^6$) and predominant 1,2,4-benzenetriyl core structures are obtained in high yields (up to 93%). Internal diynes can be polymerized into hexasubstituted hb-PAPs in moderate yields and molecular weights, probably due to the steric hindrance of the terminal groups (R).

Copolycyclotrimerization of the diynes with monoynes can be used to incorporate functional groups into the hb-PAP structure at the molecular level. This is demonstrated by the synthesis of hb-P[**1**(5)/**I**]: the hb-PAP is decorated by redox-active ferrocenyl units on its periphery [31]. We have recently found that single-component catalysts such as $TaBr_5$ and $NbBr_5$ can also initiate the polycyclotrimerization. The homopolycyclotrimerization of 1,7-octadiyne [**1**(4)] catalyzed by $TaBr_5$, for example, furnishes an hb-PAP with a high molecular weight (M_w: 5.5×10^4) in 81% yield [30].

Size exclusion chromatography (SEC) is nowadays a standard tool for the estimation of molecular weights of polymers. The SEC system calibrated with linear polymer standards such as PS, however, often underestimates molecular weights of hyperbranched polymers because of their nearly spherical topological structures [32]. Our hb-PAPs also display such a difference: their absolute M_w values are 2–7 times higher than the relative values estimated by an SEC system. The highest absolute M_w value can reach up to 3.8×10^6. Despite their high molecular weights, solutions of the hb-PAPs exhibit low intrinsic viscosities ($[\eta] < 0.2$ dL/g). The $[\eta]$ value is insensitive to the molecular weight of the polymer. This is not surprising because there is practically no chain entanglement in the hyperbranched polymer systems [20–26].

2.2. Structures

The structures of the hb-PAPs were fully characterized by standard spectroscopic methods. Fig. 1 shows examples of the ^{1}H NMR spectra of **1**(4) and its polymer hb-P**1**(4) [30]. The resonance peak of the ethynyl protons (a) of **1**(4) at δ 1.97 disappears after the polymerization, and new, broad peaks are emerged at δ 6.8–7.0 (g–m), confirming the $[2+2+2]$ polycyclization of the acetylenic triple bonds into benzene rings. The trialkylbenzene ring is formed in symmetrical 1,3,5- and asymmetrical 1,2,4-fashion with the latter being proceeded predominantly ($F_{1,2,4} = 74\%$) [30]. The propargylic protons (b) of **1**(4) are transformed into benzylic protons (f) of hb-P**1**(4), whose resonance is accordingly downfield shifted from δ 2.23 to δ 2.56.

The appearance of two peaks at δ 2.71 (e) and δ 1.76 (d) associated with back-biting reaction of the flexible diyne monomer confirms another key feature of the hb-PAP structure. The back-biting reaction plays an important role in the polycyclotrimerization of the aliphatic diynes. When this end-capping reaction is active, the propagating branches will be readily terminated, giving only oligomer products. On the other hand, if the back-biting reaction is too sluggish, the polymerization will become difficult to control, resulting in the formation of cross-linked gels. Fine tuning the back-biting

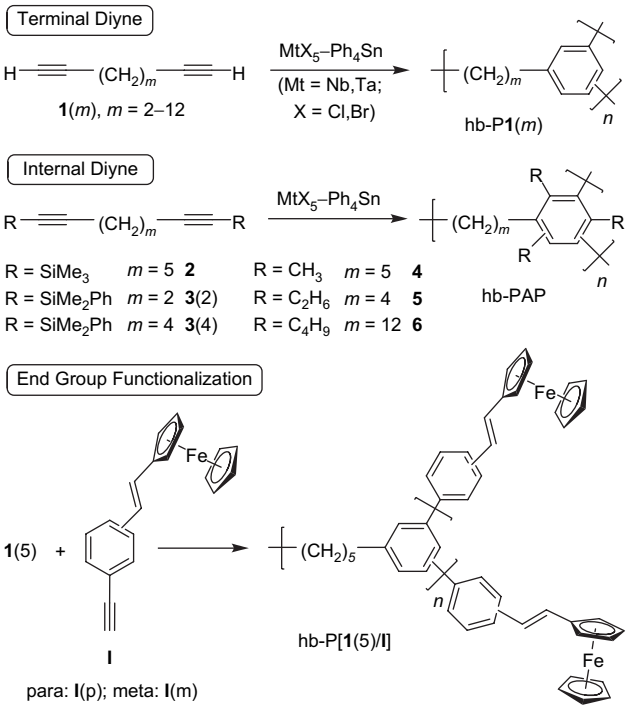

Scheme 4. Polycyclotrimerizations of terminal and internal diynes and syntheses of functional hb-PAPs end-capped by ferrocenyl groups.

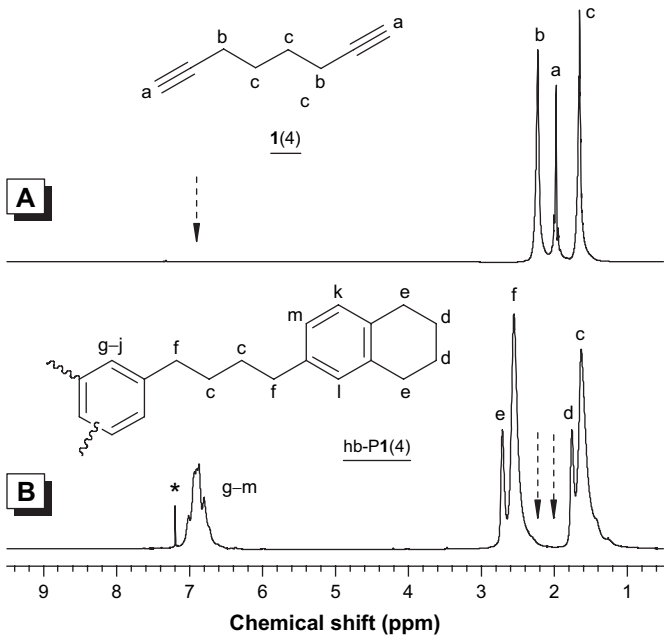

Fig. 1. ^{1}H NMR spectra of chloroform-*d* solutions of (A) 1,7-octadiyne [**1**(4)] and (B) its hyperbranched polymer [hb-P**1**(4)]. The solvent peak is marked with an asterisk.

reaction will help to control the reaction output. For example, diynes with two [**1**(2)] and three short methylene spacers [**1**(3)] have high tendency toward back-biting and form hb-PAPs with low molecular weights (Table 1, nos. 1 and 2). No terminal triple bonds but strong back-biting signals are observed in their ^{1}H NMR spectra. Diynes with long spacers [**1**(*m*), $m \geq 6$] show a low back-biting activity, which is readily confirmed by the existence of their unterminated triple bonds. As a result, the polymerizations are difficult to control, giving polymers with very high M_ws and extremely broad PDIs (nos. 5 and 7) or even totally insoluble gels (nos. 6 and 8).

An elaborate comparison of the polymerization behavior of the aliphatic diynes with different spacer lengths reveals a unique even–odd effect on their tendencies toward back-biting reaction. In the diynes with an odd number of methylene spacers, their triple bonds are in the same side, which facilitates the back-biting reaction (Scheme 5). On the other hand, in the diynes with an even number of methylene units, their triple bonds are located in the opposite sides. This unfavorable positioning hampers the back-biting reaction. Consequently, hb-P**1**(4) possesses triple bond residues in its final structure but its congener hb-P**1**(5) does not.

The hb-PAPs contain numerous branching units, resulting from the cyclization propagation and back-biting termination. In addition to the branching structures, there exists pseudo-"linear" structure in the polymers, formed by the reaction of the closely located triple bonds in a 1,2,4-substituted benzene ring (Scheme 6). The acetylene triple bonds in the 1 and 2 positions can form a new benzene ring through cyclotrimerization with another triple bond from a monomer or a polymer branch. Although this may also be considered as a "cross-linking" reaction, the structural motif is not detrimental to the solubility of hb-PAP due to its overall "linear" propagation mode. Combining all these three structural features, the hb-PAPs possess a molecular architecture resembling that of glycogen, a hyperbranched natural polymer [30].

Table 1
Analysis of the products obtained from the attempted polycyclotrimerizations of aliphatic diynes **1**(*m*) with different lengths (*m*) of methylene spacers[a]

No.	*m*	*S*[b]	Triple-bond signal[c]	Back-biting signal[c]	M_w[d]	PDI[d]
1	2	✓	Not observed	Strong	~3000	2.3
2	3	✓	Not observed	Very strong	~900	1.5
3	4	✓	Observed	Medium	~60,000	4.9
4	5	✓	Not observed	Medium	~40,000	5.0
5	6	✓	Observed	Very weak	~600,000	23.0
6	8	×				
7	9	✓	Observed	Weak	~200,000	7.9
8	10	×				

[a] Polymerization reactions carried out in toluene at room temperature under nitrogen using $TaCl_5$–Ph_4Sn as catalyst.
[b] Solubility (*S*) tested at room temperature in common organic solvents including toluene, benzene, chloroform, dichloromethane (DCM), and THF. Symbol: ✓ = soluble, × = insoluble.
[c] In the ^{1}H NMR spectrum of hb-PAP.
[d] Polydispersity index (M_w/M_n) estimated by SEC in THF on the basis of a linear PS calibration.

2.3. Properties

The hb-PAPs are thermally very stable. As can be seen from the thermogravimetric analysis (TGA) curves shown in Fig. 2, the polymers lose little of their weights when heated to a temperature as high as ~500 °C. Their thermal stabilities are much higher than those of PPA and PH, the linear polyacetylenes prepared by the metathesis polymerizations of phenylacetylene and 1-hexyne, which start to decompose at temperatures as low as ~220 and ~150 °C, respectively. Only glass transitions but no melting transitions are detected by differential scanning calorimetry (DSC) analyses of the hb-PAPs, indicative of an amorphous morphology associated with their irregular and highly branched molecular structure. The glass transition temperature (T_g) of hb-PAP is decreased with an increase in the spacer length, due to the internal plasticization effect of its flexible spacer between the benzene rings.

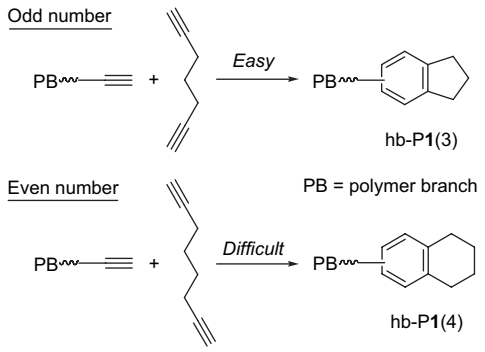

Scheme 5. Odd–even effect on the back-biting reaction in the diyne polycyclotrimerization.

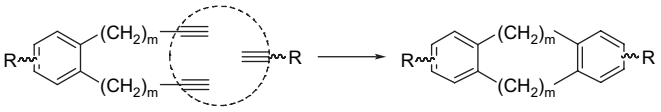

Scheme 6. Pseudo-"linear" propagation mode in the polycyclotrimerizations of aliphatic diynes.

Thin solid films of the hb-PAPs are highly transparent and absorb almost no visible light, which is easy to understand, because the polymers comprise isolated benzene rings. The thin film of hb-P**1**(5), for example, displays an optical dispersion (D) as low as 0.009 in the visible spectral region, much superior to those of the commercially important "organic glasses" such as PMMA ($D = 0.0175$) and polycarbonate (PC, $D = 0.0297$) [29].

The hb-PAPs contain many benzyl units, which readily form radical species upon photoexcitation. Recombination of the radicals should result in curing or hardening of the polymers. Indeed, thin films of the hb-PAPs are readily cross-lined upon illumination with a UV lamp. Fig. 3 shows the formation of insoluble gel upon exposure of a thin film of hb-P**1**(4) to a UV irradiation. After ~20 min exposure, almost the whole film is cross-linked with an F_g value of ~100%, indicative of a high photosensitivity of the polymer in spite of its irregular hyperbranched structure.

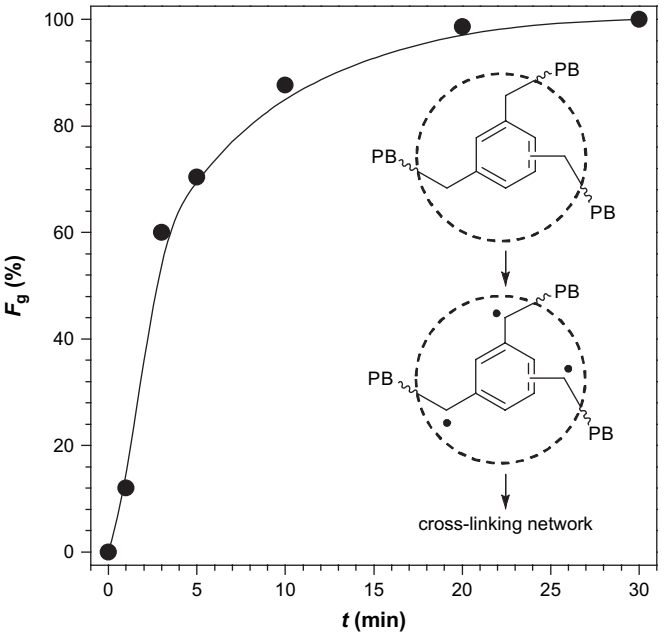

Fig. 3. Plot of gel fraction (F_g) in UV-irradiated hb-P**1**(4) film versus exposure time (t). PB stands for a polymeric branch.

3. Hyperbranched poly(arylenephenylenes) (hb-PArPs)

The exciting results described above prompted us to forge ahead in this new area of research. We replaced the saturated methylene chains in the alkyl diynes by unsaturated aromatic rings in aryl diynes. Different from the isolated benzene rings in the hb-PAPs discussed above, the new benzene rings of the hb-PArPs formed by the polycyclotrimerizations of the arylenediynes are interconnected by the "old" aromatic units from the monomers. This should endow the hb-PArPs with an extended π-conjugation and hence interesting electronic and optical properties.

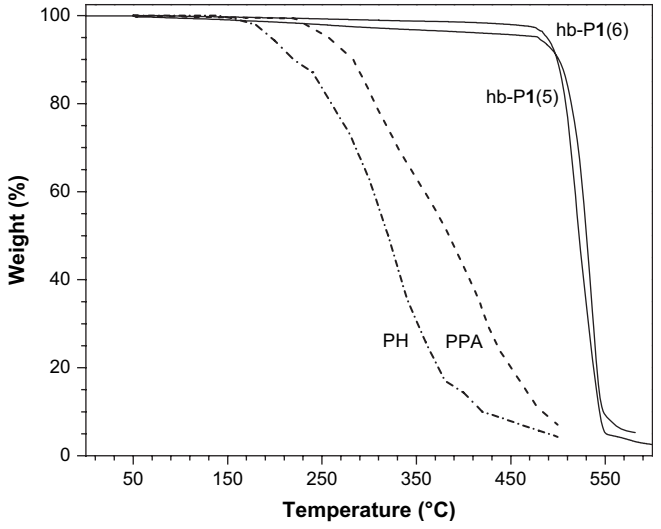

Fig. 2. TGA thermograms of hyperbranched poly(alkylenephenylenes) hb-P**1**(5) and hb-P**1**(6). Data of poly(phenylacetylene) (PPA) and poly(1-hexyne) (PH) are shown for comparison.

3.1. Synthesis

We designed and synthesized a wide variety of organic and organometallic arylenediynes as well as monoynes, examples of which are shown in Scheme 7 [33–45]. Most of the acetylenic monomers were prepared in high yields by the palladium-catalyzed cross-coupling of silylacetylenes with dihaloarenes followed by base-catalyzed desilylation. Despite their rigid molecular structures and lack of back-biting capability, the homopolycyclotrimerizations of metallolyldiynes (**26** and **27**), carbazolyldiynes (**28–31**) and silyldiynes (**36–40**) initiated by the Ta, Nb and Co catalysts proceeded smoothly, giving soluble hb-PArPs with high molecular weights in high yields [40–45]. The large free volumes and the irregular structures created by the nonplanar, nonlinear metallolyl, carbazolyl and silyl units may have conferred the excellent solubility on the homopolymers. Homopolycyclotrimerizations of other aromatic diynes including **7–25** and **32–35** all proceeded very rapidly, giving polymeric products with partial or total insolubility in common organic solvents, due to the involved cross-linking reactions.

In order to suppress the undesired cross-linking reactions in the polycyclotrimerization processes and to improve the macroscopic processability of the resultant polymers, copolycyclotrimerizations of the aromatic diynes with monoynes (**II–VIII**) were carried out. This approach worked very well: all the copolycyclotrimerization reactions proceeded smoothly with good controllability, producing completely soluble hb-PArPs with

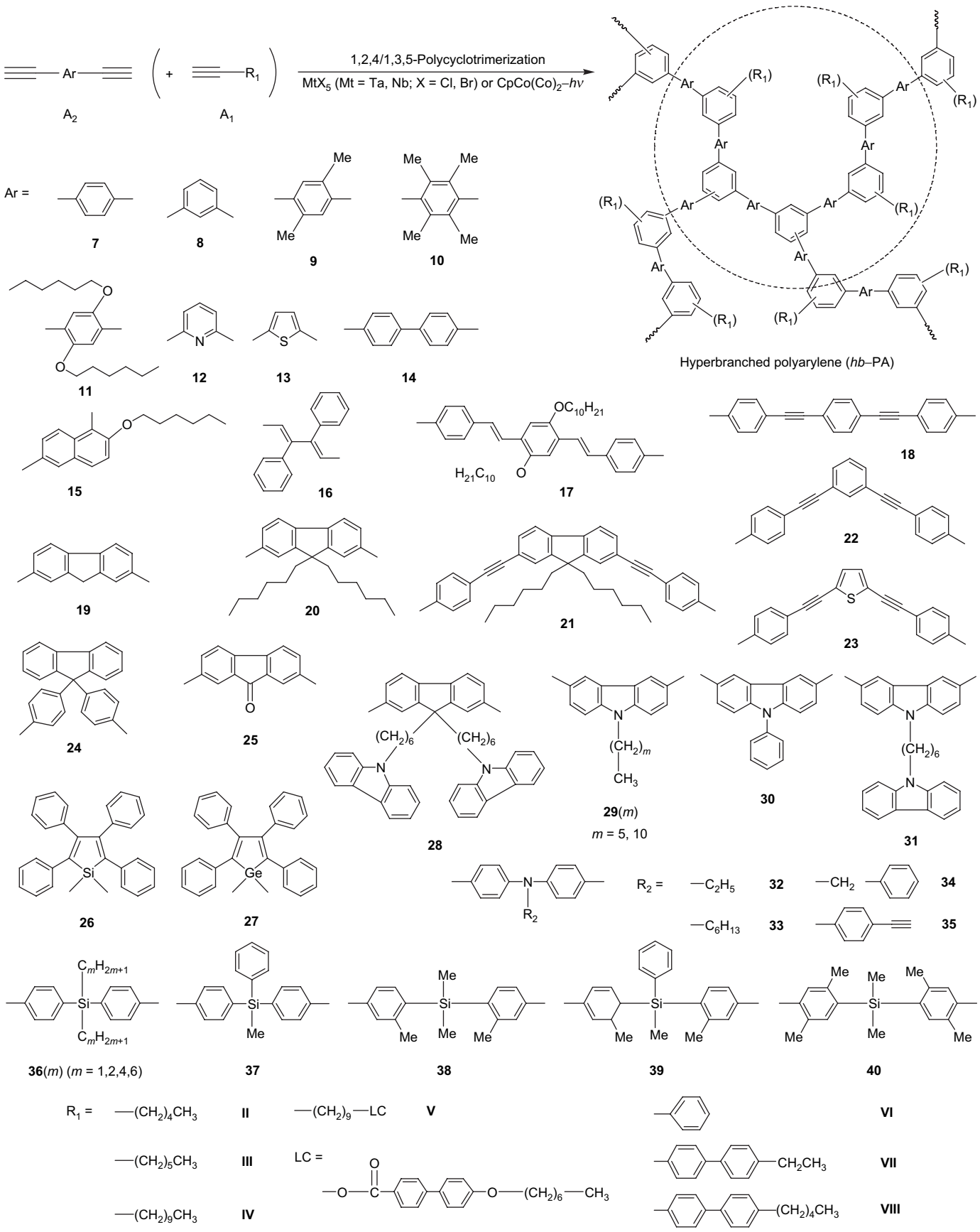

Scheme 7. (Co)polycyclotrimerizations of aromatic diynes (with monoynes).

high molecular weights (M_w up to $\sim 1.8 \times 10^5$) in high yields (up to 99.7%). Among the monoynes, 1-alkynes (**II**–**V**) are generally better comonomers than their 1-arylacetylene congeners (**VI**–**XIII**) when the molecular weights of the copolymers are concerned. This is probably due to the following effects. First, the long alkyl chains may confer higher solubility on the propagating species, hence enabling their uninterrupted, continued growth into bigger polymers. The second may be electronic effect. The electron-donating alkyl groups make the triple bonds of 1-alkynes electronically richer, which are likely to favorably interact and react with the electronically poorer aromatic diynes [46]. In other words, the donor–acceptor interactions have promoted the formation of higher molecular weight hb-PArPs from the monomer pairs of aliphatic monoynes and aromatic diynes.

3.2. Structures

Structural analyses of the homopolymers by spectroscopic methods confirm that the triple bonds of the arylenediynes have undergone [2 + 2 + 2] polycyclotrimerizations to form new benzene rings. The ratio of the 1,2,4- to 1,3,5-isomer of the trisubstituted benzene rings is estimated to be typically ~2.2:1. Careful inspection of the ^{1}H NMR spectra unveils that the number of the terminal acetylene triple bonds in the final hb-PArPs is much smaller than that in an "ideal" hyperbranched structure produced by the diyne polycyclotrimerization. This suggests that intrasphere ring formation has been involved in the polycyclotrimerization. Unfortunately, however, the signals from the newly formed benzene rings by the intrasphere cyclotrimerizations are indistinguishable from each other and also indistinct from those of the benzene rings formed by the "normal" polycyclotrimerization reactions in the ^{1}H NMR spectra, making it difficult to experimentally determine the probabilities of the intracyclotrimerization reactions.

To solve this problem, computational simulation was exercised [47]. The models of the polymers were built, and the probabilities of the growth modes were estimated according to the minimized energy of the structures. An example of the outputs of the computer simulations is shown in Fig. 4. The overall two-dimensional structure of hb-P**36**(1) looks like a star-shaped polymer containing many small cyclic units. The total number of triple bonds left in the hyperbranched structure and the total number of aromatic protons are in good agreement with the numbers estimated from the ^{1}H NMR spectral data. The computer simulation model is therefore consistent with the structure of the real polymer. Although the intracyclotrimerization occupies more than 1/3 (or 36%) of the probabilities of the propagation modes, most of the cycles are small in size, formed by only two monomer repeat units mainly due to the close proximity of the 1 and 2 positions of the newly formed 1,2,4-trisubstituted benzenes. These small rings are strung together to form willow twig-like structure, well accounting for the excellent solubility of the polymer.

Similarly, spectral characterizations of the copolymers substantiate their hyperbranched structures. Estimations of the ratios of the diynes to monoynes incorporated into the copolymer structures reveal that the monoynes function as growth-controlling agents, impeding the intracyclotrimerization reactions [44,48,49]. As an optimal ratio of diyne to monoyne, 1:1.5 has often been found to work well for most diynes to yield completely soluble, high molecular weight hb-PArPs. The copolycyclotrimerization of aromatic triynes such as **35** is inherently much more difficult to control. For the aliphatic monoynes like 1-octyne (**III**), a monoyne/triyne ratio of 3:1 is needed to obtain a soluble hb-PArP. A larger

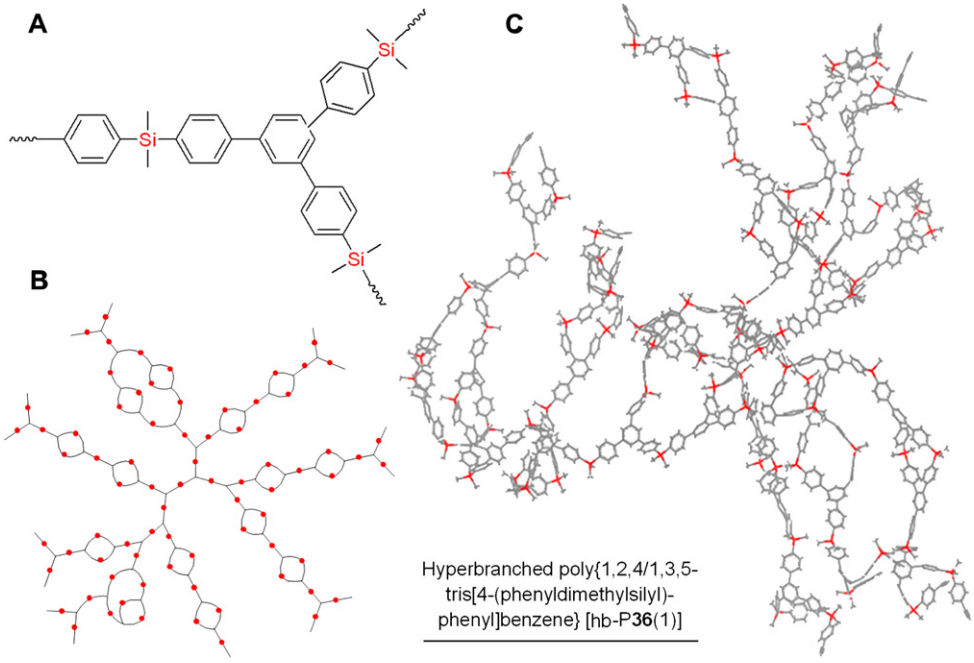

Fig. 4. (A) Chemical structure and simulated (B) two- and (C) three-dimensional topological structures of hb-P**36**(1).

monoyne to diyne ratio (4:1) is required for the aromatic monoynes such as phenylacetylene (**VI**) [48].

Even when such a large excess of growth-controlling agent of monoyne is used, the resultant hb-PArPs still contained internal cyclic structures [48]. According to the ratio of monoyne to triyne units found in hb-P(**35/III**), different propagation modes for the intrasphere cyclotrimerization reactions are proposed (Scheme 8). Taking the 1,2,4- and 1,3,5-isomeric structures of the trisubstituted benzenes into account, formation of ''small''- and ''medium''-sized cycles is highly possible. Similar to the silyldiyne homopolycyclotrimerization, the close intramolecular proximity of the two triple bonds originating from an *ortho* connection allows growth termination by the triple bond of 1-octyne, furnishing a second 1,2,4-trisubstituted benzene ring (Scheme 8A). This intrasphere ''cross-linking'' leads to the formation of a small cyclic structure, yet the polymer is still soluble due to the overall pseudo-''linear'' propagation mode.

Another possible pathway is the ring closure of three triyne monomer units connected in a *meta* fashion with a monoyne via 1,2,4- or 1,3,5-cyclization. Such a reaction is likely to produce a medium-sized ring, serving as a core for the macrodendritic propagation with three growing arms (Scheme 8B). *para*-Substituted polymer branches resulting from 1,2,4-cyclotrimerization inherently cannot form any ring structures and

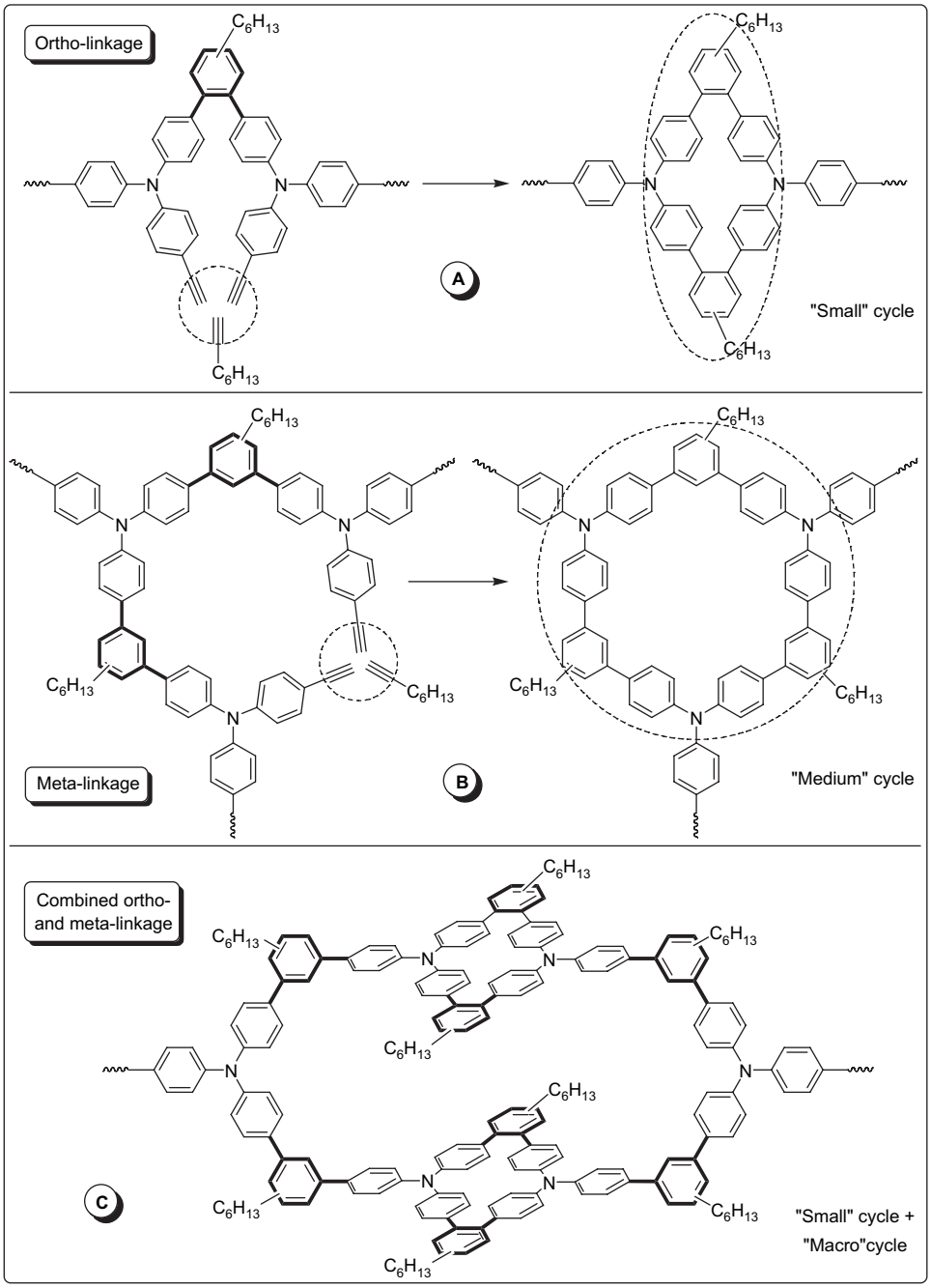

Scheme 8. Formation of intramolecular cyclic structures in triyne/monoyne copolycyclotrimerization.

may only be involved in the formation of oval-shaped "macrocycles". Such cyclic substructures are possibly formed via combined *ortho*- and *meta*-linkage (Scheme 8C), which has little effect on the solubility of the hb-PArPs, as again the overall structure is still propagating in a pseudo-"linear" mode.

3.3. Properties

The hb-PArPs comprise aromatic rings and are thus expected to be thermally stable. This is indeed the case, as proved by the TGA analyses. For example, hb-P**36**, an organosilicon hybrid polymer, loses merely 5% of its weight at a temperature as high as 595 °C (Fig. 5). Other polymers show similar performance. Most polymers graphitize in >50 wt% yields upon pyrolysis at 800 °C, with hb-P(**14/II**) carbonizing in a yield as high as 86 wt%. The thermal stabilities of the hb-PArPs are similar to that of poly(*p*-phenylene) (PPP, $T_d \sim 550$ °C) but much better than those of polyacetylenes such as PPA and PH ($T_d < 220$ °C). The difference in the thermal stability is mainly due to the difference in the molecular structure: PPP is made of thermally stable aromatic rings, whereas PPA and PH comprise labile polyacetylene chains. The outstanding thermal stabilities of the hb-PArPs thus verify their polyarylene structure comprising aromatic rings instead of polyacetylene chains.

The aromatic architecture of the hb-PArPs imparts not only outstanding thermal stabilities but also unique optical properties. Thanks to their π-conjugated structure, the polymers emit deep-blue to blue-green lights, whose intensities are higher than that of poly(1-phenyl-1-octyne), a highly luminescent polyacetylene [18]. Polymers hb-P(**7/II**), hb-P(**14/I**), hb-P(**17/II**), hb-P(**19/II**), hb-P(**19/III**) and hb-P(**28/II**) all give very high fluorescence quantum yields ($\Phi_F > 70\%$), with hb-P(**19/III**) showing a Φ_F value of almost unity (98%).

During our search for efficient light-emitting materials, we have discovered a group of nonemissive molecules called silole (**26**) and germole (**27**) whose emissions can be induced by aggregate formation, for which we coined a new term "aggregation-induced emission" [41,50,51]. We prepared hb-PArPs from the metallole-containing diyne monomers, an example of which is shown in Fig. 6. While diyne 1,1-dihexyl-2,5-bis(4-ethynylphenyl)-3,4-diphenylsilole is nonemissive, its polymer (hb-PDHTPSP) is somewhat luminescent. The emission of the polymer is enhanced by aggregate formation: the intensity of its photoluminescence is progressively increased with gradual addition of water, a poor solvent, into its dilute THF solution. This novel effect of aggregation-enhanced emission is caused by the restriction of intramolecular rotations of the phenyl rings around the axes of the metallacyclopentadiene core in the aggregation state, which efficiently blocks nonradiative decay pathways [52].

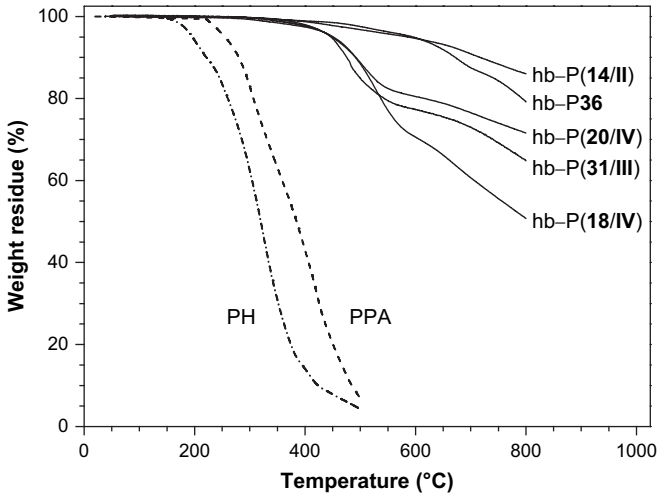

Fig. 5. TGA thermograms of hb-PArPs. Data for linear polyacetylenes of PPA and PH are shown for comparison.

The hb-PArPs are nonlinear optically active and strongly attenuate the optical power of harsh laser pulses. As shown in Fig. 7, in the low energy region, the fluence transmitted from a solution of hb-P(**18/IV**) linearly increases with an increase in the incident fluence. The transmitted fluence, however, starts to deviate from the linearity at an incident fluence of ~250 mJ/cm^2 and reaches a saturation plateau of ~140 mJ/cm^2. The optical limiting performance of hb-P(**18/IV**) is superior to that of C_{60}, a well-known optical limiter [53,54]. Taking into account that C_{60} is a three-dimensionally π-conjugated buckyball, it may be concluded that the three-dimensionally π-conjugated electronic structure of the hb-PArPs is responsible for their optical limiting properties. Compared to hb-P(**18/IV**), hb-P(**21/IV**) is a better optical limiter (with a saturation plateau as low as ~50 mJ/cm^2) but P(**19/III**) is a poorer one [33]. Clearly, the optical limiting power of the hb-PArP is sensitive to a change in its molecular structure, thus offering the opportunity to tune its performance through molecular engineering endeavor.

4. Hyperbranched poly(aroylphenylenes) (hb-PAkPs) and poly(aroxycarbonylphenylenes) (hb-PAePs)

The hb-PAPs and hb-PArPs discussed in Sections 2 and 3 are both synthesized from transition metal-catalyzed alkyne polycyclotrimerizations. Due to the coordination nature of the metal-catalyzed polycyclotrimerization reactions, the resultant polymers possess regiorandom structures consisting 1,3,5- and 1,2,4-trisubstituted benzene isomers. The structural irregularity may not be disadvantageous for some practical applications and is actually beneficial to the enhancement in the solubility and hence processability of the polymers. This, however, makes it a challenging job to completely characterize the molecular structures of the polymers by spectroscopic methods. Furthermore, the Ta- and Nb-based catalysts are highly air- and moisture-sensitive and intolerant of polar functional groups. The residues of the metallic catalysts, which are difficult to completely remove from the polymerization products, are detrimental to the properties, especially the optical and photonic activities, of the polymers. It would be nice if an acetylene polycyclotrimerization can proceed in a regioselective manner in the absence of metallic catalysts. We thus explored the possibility of developing metal-free, regioselective acetylene polycyclotrimerization reactions.

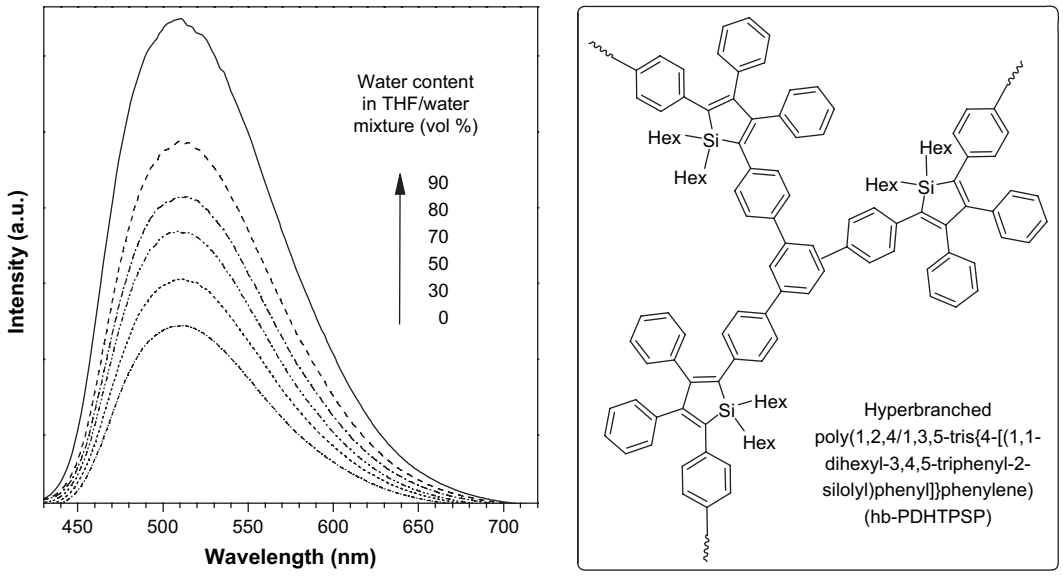

Fig. 6. Photoluminescence spectra of hb-PDHTPSP in THF/water mixtures with different water contents; polymer concentration: 10 μM.

4.1. Synthesis

We noted that benzoylacetylene could be cyclotrimerized to form 1,3,5-tris(phenylcarbonyl)benzene in the presence of diethylamine or when refluxed in *N*,*N*-dimethylformamide (DMF) [55]. We tried to develop this reaction into a new polycyclotrimerization technique for the synthesis of 1,3,5-regioregular hyperbranched polymers from functionalized acetylenes. We prepared a series of bis(aroylacetylene)s with various linkers (R; Scheme 9) and studied their polymerization behaviors. None of the catalysts, however, worked well for the polycyclotrimerizations of the bis(aroylacetylene)s: the reactions in the presence of diethylamine gave polymers in very low yields (down to 7%), while those carried out in refluxing DMF/tetralin mixtures were sluggish, taking as long as 3 days to get some satisfactory results.

We thus searched for new catalysts and eventually found that piperidine was a good organocatalyst. The reactions catalyzed by piperidine completed in shorter times and produced polymers in much higher yields: for example, the polycyclotrimerizations of **41**(6) and **43**(4) initiated by piperidine produced their corresponding polymers, i.e., hb-P**41**(6) and hb-P**43**(4), in virtually quantitative yields in 24 h [56]. Spectroscopic analyses prove that the aroyldiynes are regioselectively polycyclotrimerized by piperidine into hb-PAkPs with 1,3,5-conformation. This regioselectivity stems from ionic, instead of coordinative, mechanism of the base-catalyzed polycyclotrimerization where piperidine reacts with an aroylethynyl group in a Michael addition mode via the formation of ketoenamines [56].

The bis(aroylacetylene)s are, however, difficult to prepare. It takes many steps of reactions to get the products. If the carbonyl linkage between the triple bond and aromatic ring in the bis(aroylacetylene) can be replaced by an ester group, it will make the monomer synthesis much easier. Propiolic acid (or acetylenecarboxylic acid) is a commercially available compound and can be readily esterified with diols to form bipropiolates. We designed and prepared a group of arylene bipropiolates by the esterification of propiolic acid with arylene diols in the presence of *N*,*N*′-dicyclohexylcarbodiimide (DCC), 4-dimethylaminopyridine (DMAP) and *p*-toluenesulfonic acid (TsOH), examples of which are shown in Scheme 10.

To examine whether the arylene bipropiolates could be polycyclotrimerized, we conducted a model reaction using a monoyne of phenyl propiolate as model compound and found that it readily underwent 1,3,5-cyclotrimerization in refluxing DMF. Based on the result of the model reaction,

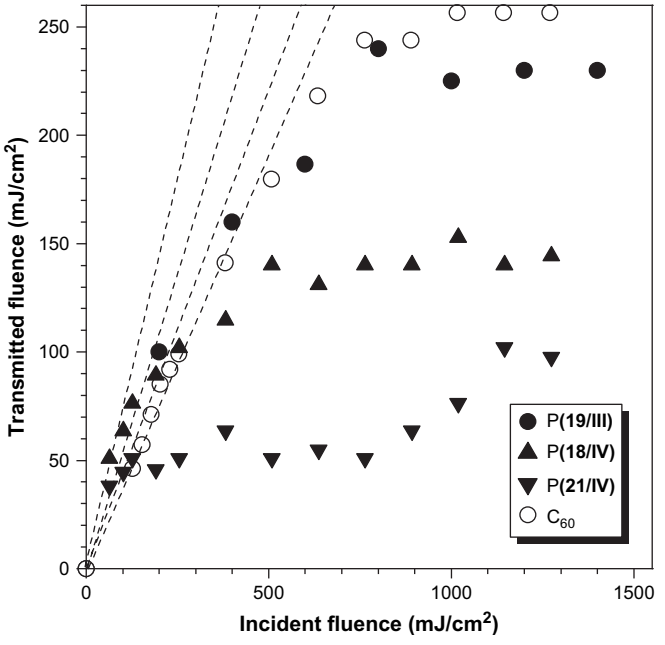

Fig. 7. Optical limiting responses to 8 ns, 532 nm optical pulses, of DCM solutions (0.86 mg/mL) of hb-PArPs. Data for a toluene solution of C_{60} (0.16 mg/mL) is shown for comparison.

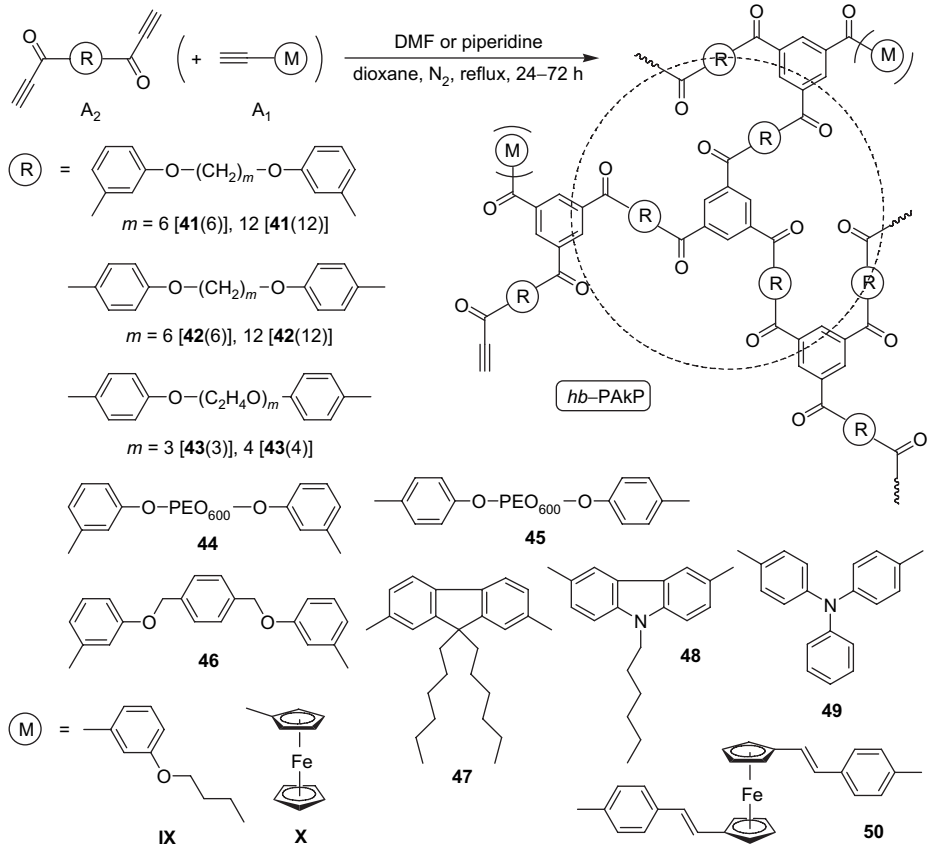

Scheme 9. Metal-free, 1,3,5-regioselective polycyclotrimerization of bis(aroylacetylene)s.

we carried out polycyclotrimerization reactions of the arylene bipropiolates in refluxing DMF and succeeded in the transformation of the monomers into their corresponding polymers hb-PAePs in a 1,3,5-regioselective fashion [57]. The polymerization can even be conducted in air: for example, heating **52** in reflux DMF in air for 24 h gives an hb-P**52** with a molecular weight of 13,200 in 82% yield. We also found that the bipropiolate monomers could be readily polycyclotrimerized by organoruthenium complexes such as $Cp^*Ru(PPh_3)_2Cl$, $CpRu(PPh_3)_2Cl$, $Ru(OAc)_2(PPh_3)_2$ and $[RuCl_2(allyl)_2]_2$ {e.g., dichlorobis(μ-chloro)bis[(1-3-η:6-8-η)-2,7-dimethyloctadienediyl]diruthenium(IV)}. The polycyclotrimerization of **51** catalyzed by $Cp^*Ru(PPh_3)_2Cl$ in THF at room temperature, for example, produced an hb-P**51** with a molecular weight of 12,100 in 78% yield in a reaction time as short as 2 h.

4.2. Structures

Hyperbranched structures of the hb-PAkPs and hb-PAePs are readily confirmed spectroscopically. Thanks to the 1,3,5-

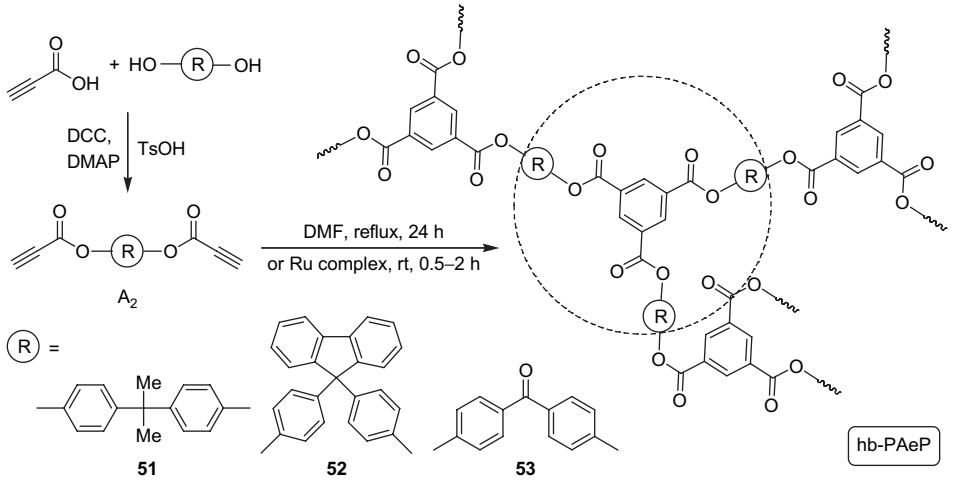

Scheme 10. 1,3,5-Regioselective polycyclotrimerization of arylene bipropiolate monomers catalyzed by nonmetallic or metallic catalysts.

regioregularity of the polymer structure endowed by the regioselectivity of the diyne polycyclotrimerization, the NMR spectra of the polymers are much simpler, in comparison to those of their hb-PArP congeners. The presence of three basic structures of an hb-PAkP, viz., *D*, *L* and *T* units, is readily verified by the numbers of unreacted triple bonds in the repeat branches (Scheme 11).

Due to the structural flexibility of the monomers, especially **41**–**45**, the polymer branches can also be terminated by an additional end-capping reaction of dimerization, in which two triple bonds of the same diyne molecule react with a ketoenamine to form a new benzene ring. The end group resulting from this back-biting reaction is called "cyclophane terminal" (T_c). From their corresponding resonance peaks in the ^{1}H NMR spectra, the degree of branching of the polymers (DBs) are estimated to be 78–100%. These DB values are much higher than those of the "conventional" hyperbranched polymers, which are commonly in the neighborhood of 50% [58].

4.3. Properties

The great advantage of these systems is that they do not suffer from any metallic residues left behind after polymerizations because the catalysts and solvents can be removed from the polymer products with ease. Taking advantage of this

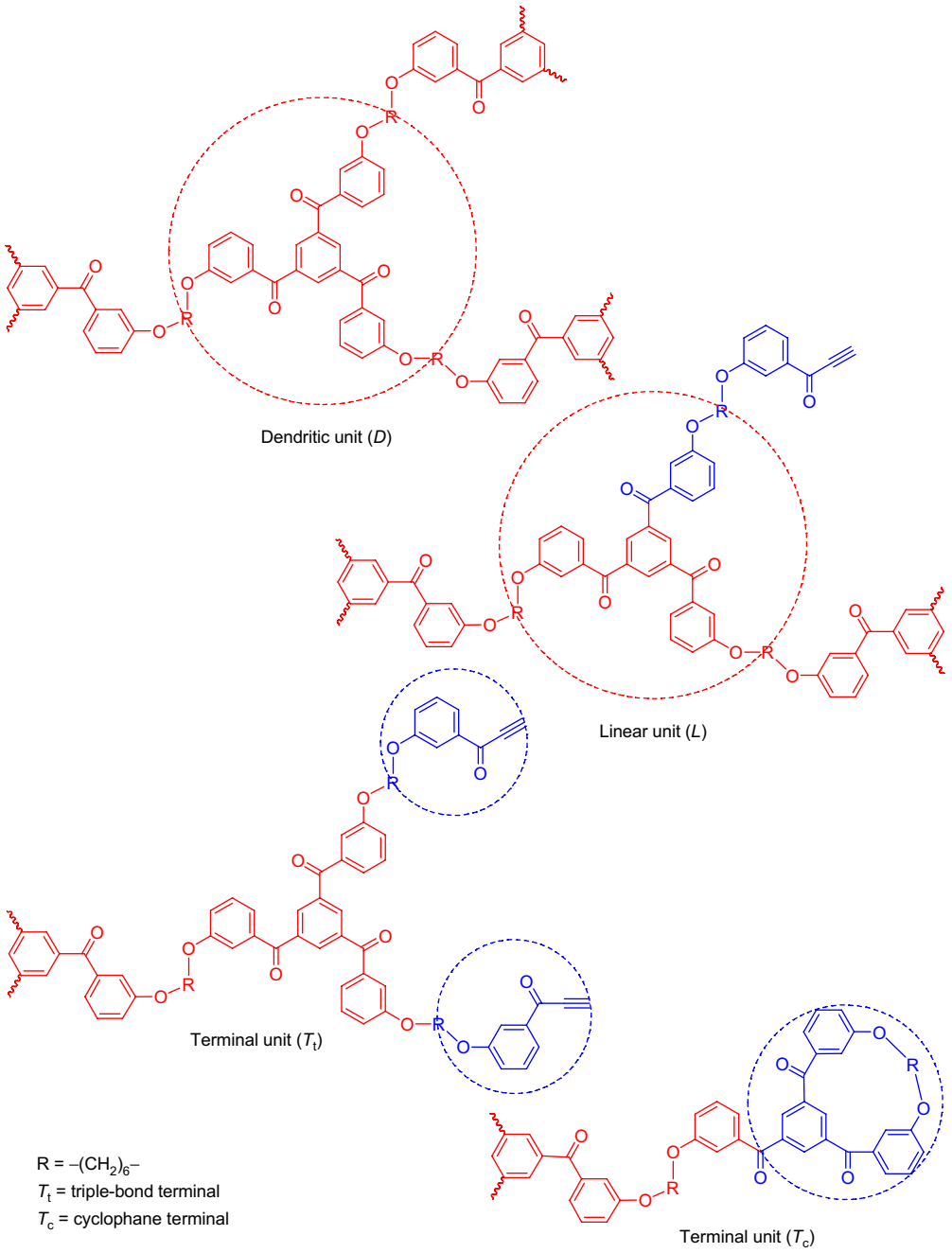

Scheme 11. Structures of *D*, *L* and *T* units in hb-P**41**(6).

process feature, we generated three-dimensional polymer nanostructures by carrying out the diyne polymerizations in the presence of an anodic aluminum oxide (AAO) template. The nanostructured polymers were freed by breakage or dissolution of the AAO template in aqueous sodium hydroxide solutions. Examples of the scanning electron microscopy (SEM) images of such a polymer, hb-P**41**(6), are shown in Fig. 8. The hb-PArP adopts well the shapes and sizes of the pores of the template and formed micrometer-long polymer nanotubes, as can be clearly seen from the image given in Fig. 8D.

Due to its high photosusceptibility, benzophenone has been introduced into biological and synthetic polymers to serve as a photo-cross-linking agent, and its photoreactions in various polymer matrixes such as PS, PMMA and PC have been well documented [59]. The hb-PAkPs contain numerous aroylbenzene units and are thus expected to show high photo-cross-linking efficiencies. Indeed, when a thin film of hb-P**46** on a glass plate is exposed to a hand-held UV lamp at room temperature, it is readily cross-linked. The cross-linking reaction may have proceeded via a well-established radical mechanism [59]: the carbonyl groups abstract hydrogen atoms from the benzyl units to generate benzyl radicals, whose coupling or combination leads to cross-linking and hence gel formation [56].

Fig. 9A shows the effect of radiation dose on the gel formation of hb-PAkP films after they have been exposed to a weak UV light with a power of $\sim$1 mW/cm^2. Although the photoreaction conditions have not been optimized, the polymers already exhibit much higher sensitivities ($D_{0.5} = 43-180$ mJ/cm^2) than those of commercial poly(amic ester)-based photoresists ($D_{0.5} = 650-700$ mJ/cm^2) [60]. Well-resolved patterns with line widths of $\sim$1.0 μm are readily formed when a film of hb-P**46** is exposed to a UV dose of 1 J/cm^2. Patterns with submicron resolutions (line width down to 500 nm) are also achieved, as demonstrated by the example given in Fig. 9D. Evidently, hb-P**46** is an excellent photoresist material.

Our previous studies have shown that hyperbranched organometallic polymers containing ferrocenyl units can be transformed into nanostructured magnetic ceramics in high yields [61–63]. The ferrocene-containing hb-PAkPs synthesized in this study are thermally stable and photonically cross-linkable. We envision that the hb-PAkPs may be used to create magnetic patterns. We developed a two-step process for the pattern generation. In the first step, microstructured patterns are created by developing a thin film of hb-P**46**X in 1,2-dichloroethane, after the polymer film has been exposed to a UV irradiation through a copper negative mask for 30 min (Fig. 10A). In the second step, the organometallic patterns are transformed into magnetic ceramics by pyrolyzing the microgrids at 1000 °C for 1 h under nitrogen. As can be seen from Fig. 10B, the negative-tone photoresist has been successfully transformed into well-defined and fine-patterned iron-containing ceramics with excellent shape retention. The patterned ceramic has been found to exhibit unique soft ferromagnetism.

5. Hyperbranched polytriazoles (hb-PTAs)

Acetylenes and azides can undergo 1,3-dipolar cycloaddition to form triazoles. This reaction has recently been promoted by Sharpless et al. as ‘‘click chemistry’’ [64]. Researchers have tried to prepare hb-PTAs by ‘‘click polymerization’’ of AB_2-type monomers, where A and B denote azide and acetylene groups, respectively [65]. The azidodiyne monomers carrying mutually reactive acetylene and azide groups are, however, difficult to prepare and handle and can self-polymerize into regiorandom hb-PTAs at room temperature. Attempts to control the polymer structure by using Cu(I) as catalyst yielded

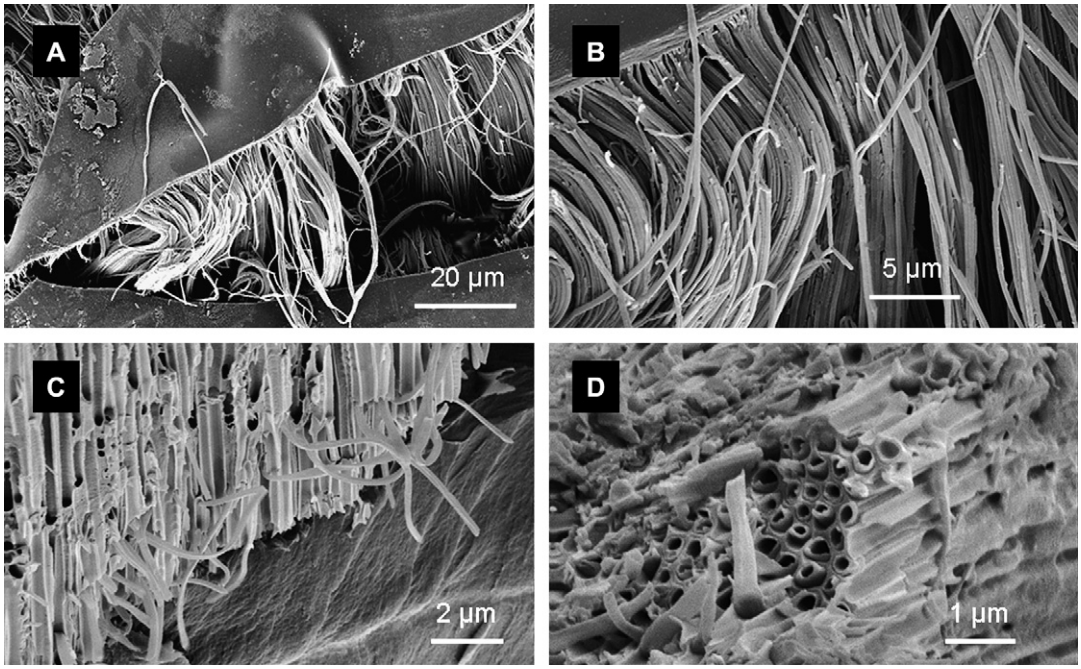

Fig. 8. SEM micrographs of the nanotubes of hb-P**41**(6) prepared inside an AAO template with a pore size of $\sim$250 nm.

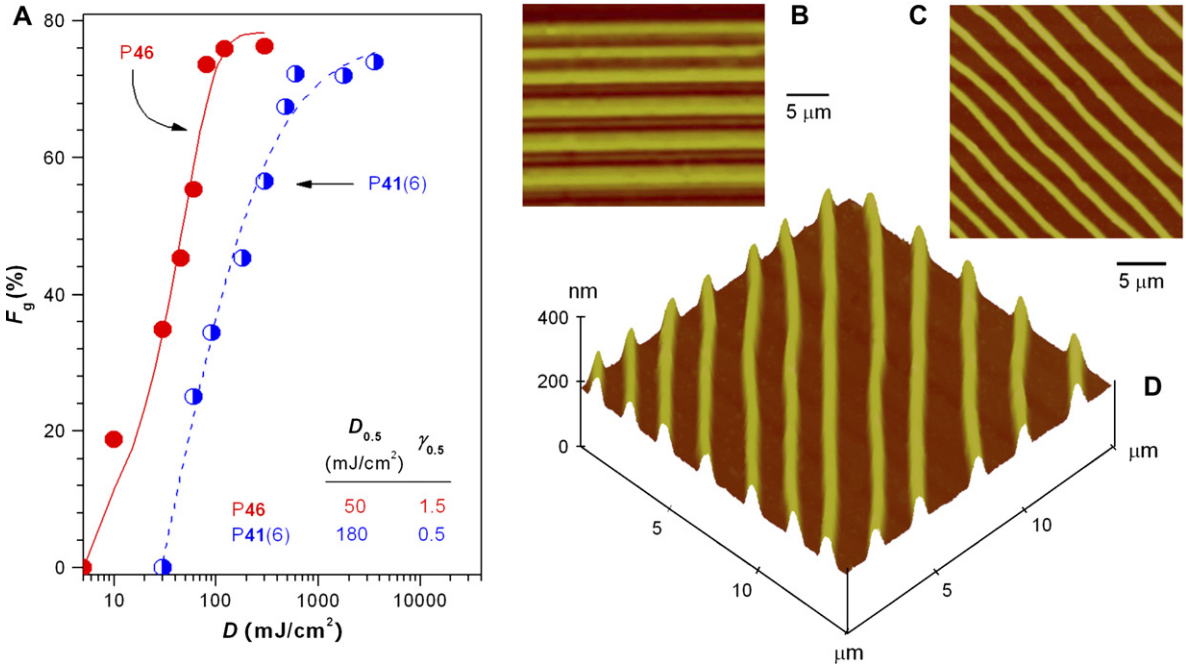

Fig. 9. (A) Plots of gel fractions (F_g) of hb-P**41**(6) and hb-P**46** films versus exposure doses (D). (B–D) Atomic force microscopy images of micro- and nano-scale patterns obtained from the thin films of hb-P**46** exposed to 1 J/cm^2 of UV irradiation ($\lambda = 365$ nm).

1,4-regioregular hb-PTAs but the polymers were insoluble. Clearly, new systems need to be developed for the synthesis of hb-PTAs with macroscopic processability.

5.1. Synthesis

We rationalize that one possible way to gain process control and to prevent self-polymerization from occurring is to put the acetylene and azide functional groups into different monomers. This will make the preparation and purification of the monomers easier and meanwhile help to extend their shelf-lives. A series of diazides and triynes were thus prepared and then tested as monomers for click polymerizations (Scheme 12). Thermally induced 1,3-dipolar polycycloadditions of the diazides with the triynes yielded regiorandom but soluble hb-PTAs [66]. The thermal click polymerizations are, however, slow, taking 3 days to produce some appreciable amounts of polymeric products, although they are faster than the self-polymerizations of the AB_2 monomers [65] and the linear 1,3-dipolar polycycloadditions of the $A_2 + B_2$ monomers [67–69], which take more than 1 week, sometimes as long as 10 days, to produce some satisfactory amounts of polymers.

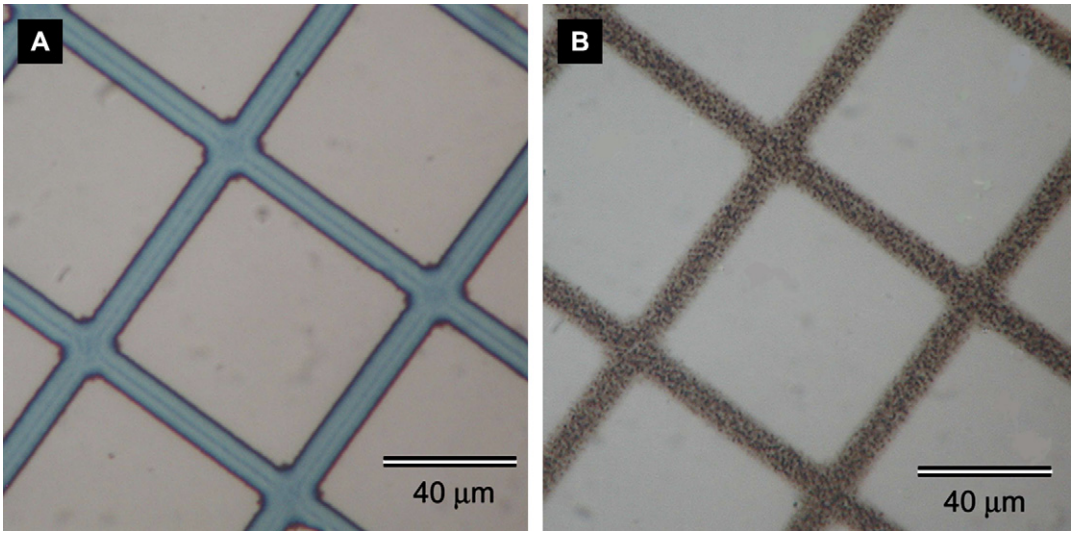

Fig. 10. Photos of (A) the micropattern fabricated by the photolysis of ferrocene-containing hb-P**46**X and (B) the magnetic pattern generated by the pyrolysis of the micropattern under nitrogen at 1000 °C.

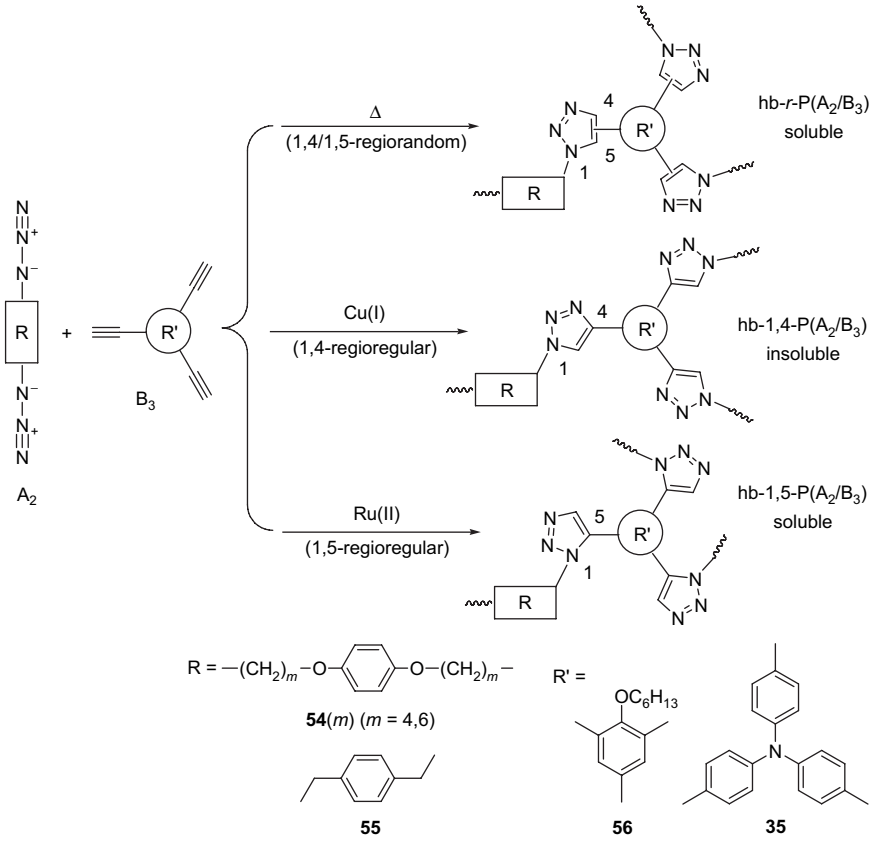

Scheme 12. Syntheses of hb-PTAs by click polymerizations.

Similar to the AB_2-type monomers discussed above, the $A_2 + B_3$ monomers can also be polymerized by the copper(I)-catalyzed click reaction into 1,4-regioregular polymers but the resultant hb-1,4-PTAs are again insoluble in common organic solvents. Isomerically pure yet completely soluble hb-PTAs with a sole 1,5-regiostructure are successfully synthesized when $Cp^*RuCl(PPh_3)_2$ is used as catalyst. The ruthenium(II)-catalyzed click polymerization proceeds very rapidly, giving an hb-1,5-PTA with a molecular weight of 9400 in 75% yield in as short as 30 min.

5.2. Structures

One possible reason for the insolubility of the hb-1,4-PTAs may be due to the in situ complexation of the copper(I) catalyst with the triazole rings formed in the click polymerization, which has cross-linked the hb-1,4-PTA spheres [70]. This process is unlikely to occur in the Ru(II)-catalyzed system. Another possible cause for the difference in the polymer solubility is the difference in the architectural structures of the 1,4- and 1,5-disubstituted triazole rings. As can be seen from the computer-simulated conformations of the model compounds given in Fig. 11, the 1,4-triazole ring experiences little steric interaction with the neighboring phenyl ring and can thus take a relatively planar confirmation. On the other hand, the steric repulsion between the 1,5-triazole and phenyl rings is strong, which forces the 1,5-isomer to adopt a more twisted molecular conformation. The structural planarity of the 1,4-isomer may facilitate π–π stacking of the aromatic units, thus making the polymer difficult to dissolve.

5.3. Properties

The hb-PTAs are light-emitting, film-forming, and photonically curable. Utilizing these properties, we tried to use the polymers to create fluorescent images. The negative-tone pattern generated by the photolysis of the regiorandom hb-*r*-PTA containing triphenylamine core, i.e., hb-*r*-P[**54**(4)/**35**], emits a white light, whereas the pattern generated by its regioregular congener, hb-1,5-P[**54**(4)/**35**], gives blue fluorescence (Fig. 12). The polymers are synthesized from the same comonomer pairs of **54**(4) and **35** and are different only in the regioisomeric structures of their repeat branches. It is truly remarkable that this seemly small change in the molecular structure has brought about such a big change in the light-emitting behaviors of the polymers. Evidently, the structural alteration in the disubstitution has resulted in changes in the effective conjugation lengths and the packing modes of the polymers, which offers a new means for fine tuning photonic and electro-optical properties of the hyperbranched polymers in the technologically useful solid state.

6. Hyperbranched poly(aryleneethynylenes) (hb-PAEs)

Repetitive coupling of acetylenes with aryl halides is another effective way to build hyperbranched architecture. This

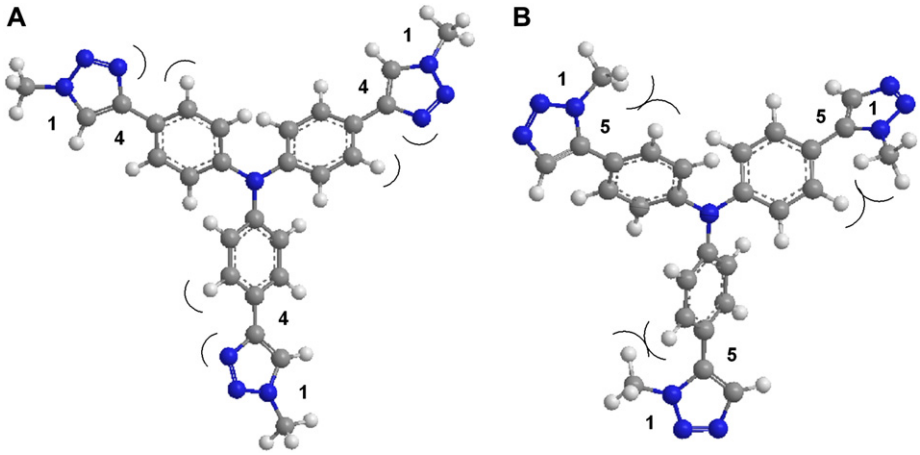

Fig. 11. Simulated conformations of model compounds with (A) 1,4- and (B) 1,5-disubstitution patterns: (A) tris[4-(1-methyl-1,2,3-triazol-4-yl)phenyl]amine (1,4-isomer) and (B) tris[4-(1-methyl-1,2,3-triazol-5-yl)phenyl]amine (1,5-isomer).

type of polycoupling is often catalyzed by palladium complexes in the presence of amines and has been widely used for the preparation of linear polymers and perfect dendrimers [71,72]. Employing this reaction protocol, hb-PAEs have been prepared from AB_2-type monomers [73,74]. Putting mutually reactive halide and acetylene groups into a single monomer is, however, a nontrivial job due to the involved synthetic problems such as undesired self-oligomerization. Purification of the desired monomers is often troublesome and ends with low isolation yields. Separation of the halide and acetylene functional groups into different monomers allows easier synthetic access and offers a greater variety of monomer choices but meanwhile invites the risk of cross-linking reactions [75]. Control of the polycoupling conditions is thus a necessity if one intends to synthesize processable hb-PAEs with desired structures and properties.

6.1. Synthesis

We worked on the optimization of polycoupling conditions by varying parameters such as reaction time, monomer concentration, and addition mode of comonomers, in an effort to control the polymer structures and to obtain soluble polymeric products. Under the optimized conditions, soluble hb-PAEs containing luminophores such as anthracene- and fluorene-functionalized hb-P(**57**/**58**) are obtained from the cross-coupling polymerization of diyne **57** with triiodide **58** (Scheme 13) [76]. Similarly, soluble hb-PAEs functionalized by azo-cored push–pull nonlinear optical (NLO) chromophores were obtained from the palladium-catalyzed polycoupling of diethynylazobenzene **59** with triiodoarenes **60** and **61** [77].

6.2. Properties

Second-order NLO materials have attracted much attention due to their photonic applications. A major effort in the area is to efficiently translate large molecular first hyperpolarizability value into high second harmonic generation (SHG) coefficient (d_{33}). The greatest obstacle has been the chromophoric aggregation in the thin films. The NLO dyes are usually highly polarized by the push–pull interactions. During the film formation, the chromophores with large dipole moments tend to compactly pack owing to the strong intermolecular electrostatic interactions, leading to the diminishment or cancellation of the NLO effects in the solid state [78]. Hyperbranched polymers should be ideal matrix materials as they offer three-dimensional spatial

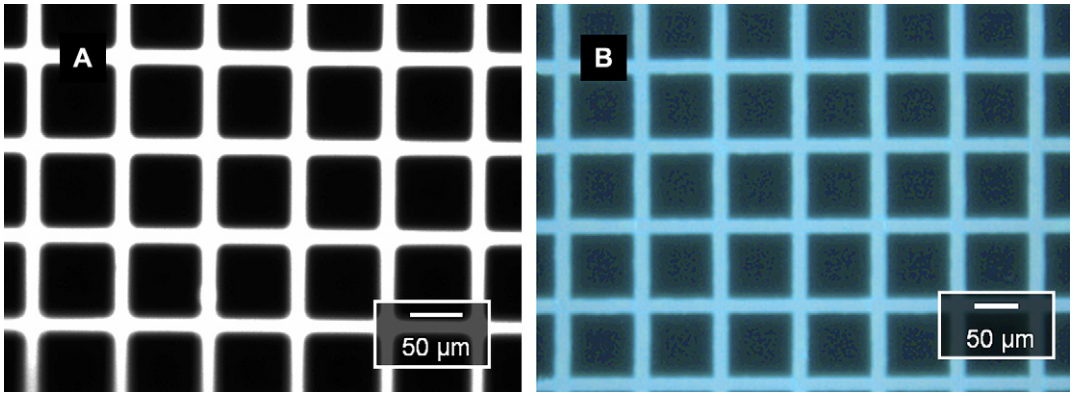

Fig. 12. Negative patterns generated by photolyses of (A) hb-*r*-P[**54**(4)/**35**] and (B) hb-1,5-P[**54**(4)/**35**]; photos taken under a fluorescence microscope.

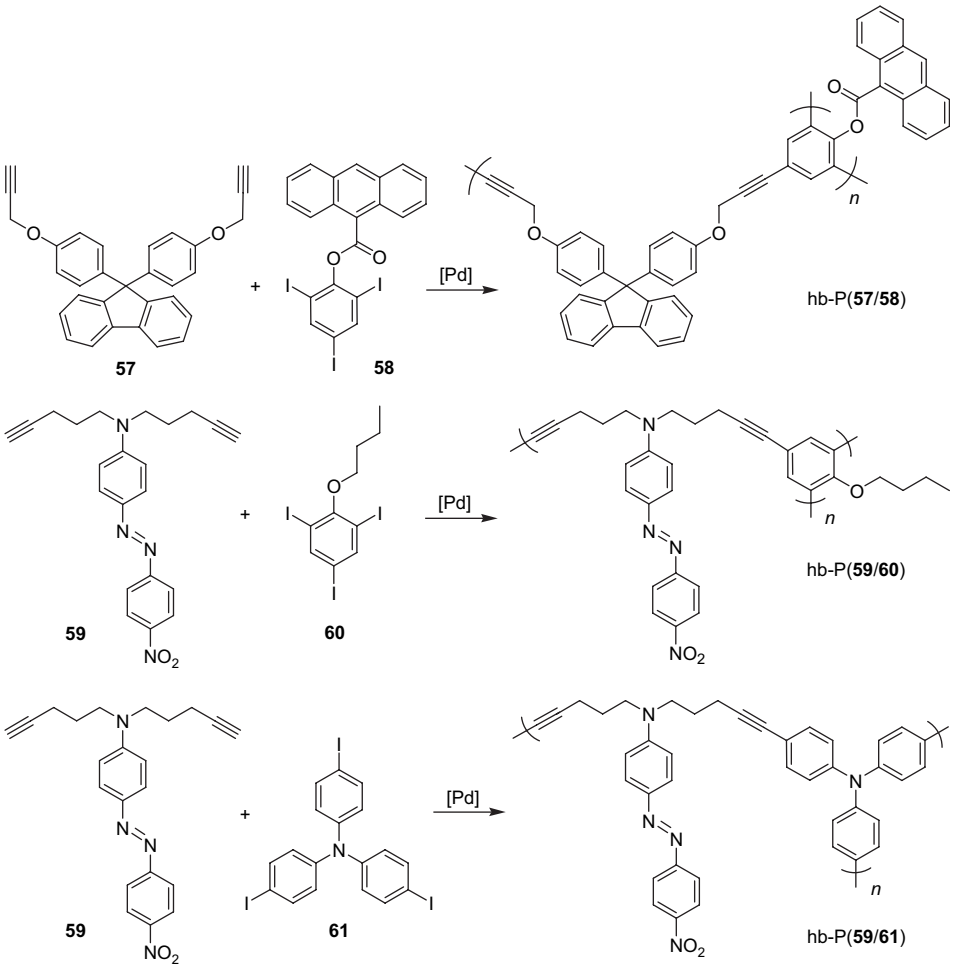

Scheme 13. Syntheses of functionalized hb-PAEs by cross-coupling polymerization.

separation of the NLO chromophores in the spherical architecture, and their void-rich topological structure should help to minimize optical loss in the NLO process.

The hb-PAEs containing the NLO-active azo dyes are film-forming and morphologically stable ($T_g > 180$ °C). Their poled thin films exhibit high SHG coefficients (d_{33} up to 177 pm/V), thanks to the chromophore-separation and site-isolation effects of the hyperbranched structures of the polymers in the three-dimensional space (Fig. 13) [77]. The optical nonlinearity of the poled film of hb-P(**59/61**) is thermally stable with no drop in d_{33} observable when heated to a temperature as high as 152 °C, due to the facile cross-linking of the multiple triple bonds in the hb-PAE at a moderate temperature of 88 °C.

7. Hyperbranched polydiynes (hb-PDYs)

The hb-PAEs discussed above possess only isolated triple bonds. We are interested in the synthesis of hb-PDYs containing two triple bonds in one repeat unit, because such polymers may exhibit novel properties associated with the diyne functionality. The rich reactivity of the diyne group, for example, may endow the hb-PDYs with photosusceptibility, thermal curability, and metal-coordinating capability. To synthesize the hb-PDYs, we took an A_3 homo-coupling approach: we

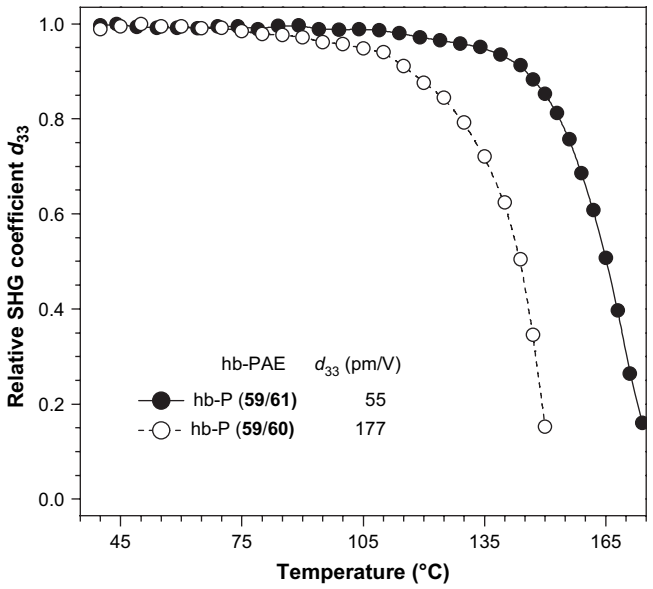

Fig. 13. Decays of SHG coefficients of hb-PAEs as a function of temperature.

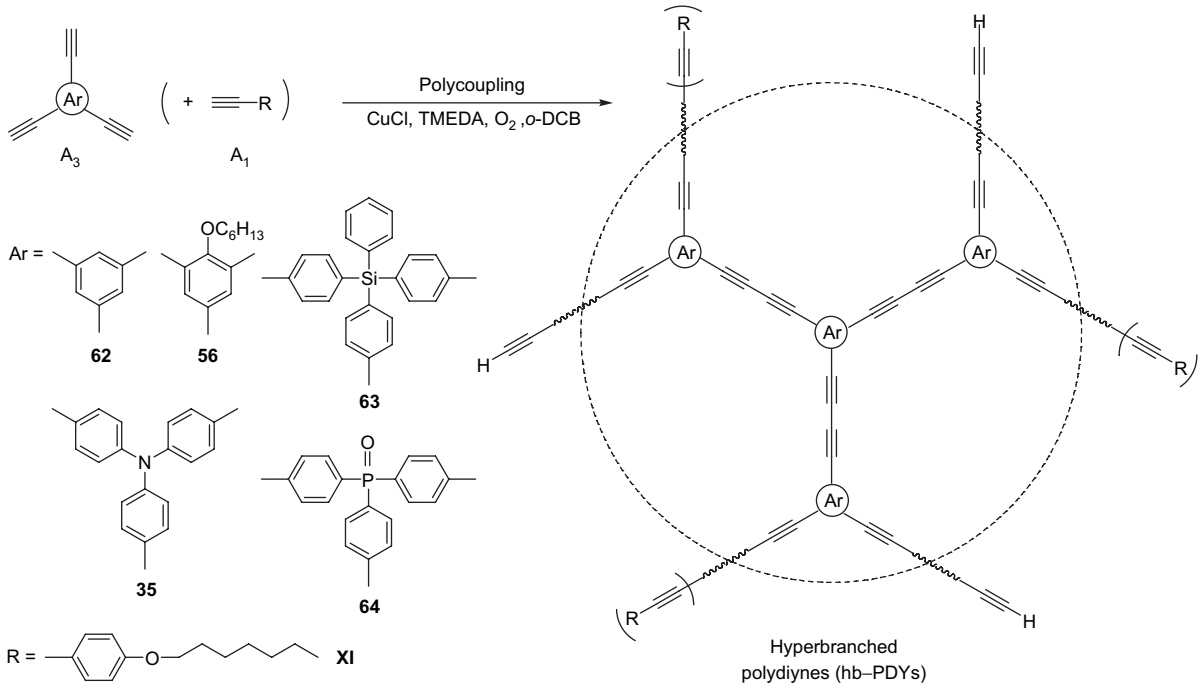

Scheme 14. (Co)polycoupling of triynes A_3 (with monoyne A_1).

knitted triyne monomers by using an oxidative polycoupling methodology [79].

7.1. Synthesis

Carbon-rich hb-PDYs containing functional groups such as ether, amine and phosphorous oxide are readily synthesized from homo-polycoupling of their corresponding aromatic triyne monomers (Scheme 14) [80]. To prevent network formation by uncontrolled cross-linking, the polymerization reactions are terminated by pouring the reaction mixtures into acidified methanol before they reaches the gel points. Another way to ensure solubility is to copolymerize the triynes with appropriate amounts of monoynes such as **XI**.

Spectroscopic analyses reveal that both the homo- and copolymers contain terminal monoyne triple bonds, which enable the peripheries of the hb-PDYs to be decorated by end-capping reactions. This is demonstrated by the coupling of hb-P**35** with aryl iodides **XII** and **XIII** (Scheme 15). The polymer end-capped by phenyl groups (hb-P**35**-**XII**) becomes only partially insoluble after purification, possibly due to the π−π stacking-induced supramolecular aggregation during precipitation and drying processes of the product of polymer reaction. Product hb-P**35**-**XIII** is, however, completely soluble, thanks to the long *n*-dodecyloxy group of the end-capping agent. No signal of resonance of the terminal acetylene proton is observed in the ^{1}H NMR spectrum, confirming the completion of the end-capping reaction.

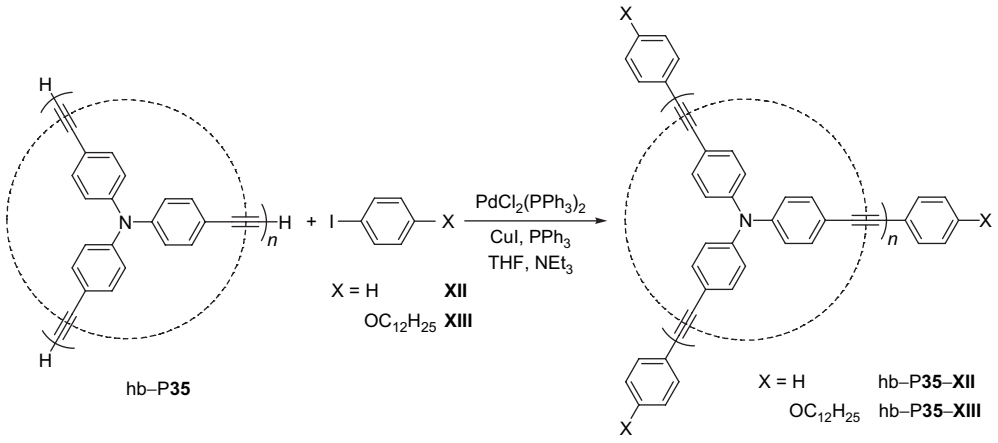

Scheme 15. Peripheral end-capping through terminal acetylene coupling with aryl iodide.

7.2. Thermal curing

Diyne molecules readily oligomerize upon heating [16]. Many prepolymers carrying monoyne end groups have been transformed into thermoset networks [81]. The hb-PDYs contain diyne groups in the cores and monoyne groups on the shells and are thus expected to be thermally curable. When hb-P**63**-**XI** is heated in a DSC cell, it starts to release heat at ~200 °C due to the commencement of thermally induced cross-linking reactions (Fig. 14). The second heating scan of the DSC analysis gives almost a flat line parallel to the abscissa in the same temperature region, suggesting that all the acetylene triple bonds have reacted during the first heating scan. The cross-linking reaction of hb-P**35** starts from ~150 °C and peaks at ~204 °C. The homopolymer begins to cure at lower temperatures in comparison to its copolymer congener, because the former carries more reactive terminal acetylene triple bonds. When the terminal acetylene groups of hb-P**35** are fully end-capped by phenyl groups, the resultant hb-P**35**-**XII** contains only internal acetylene groups, which needed higher temperatures to initiate and complete its thermal curing reactions. This further manifests the effect of the acetylene reactivity on the thermal curability of the hb-PDYs.

7.3. Micropattern formation

The diyne units can be induced to cross-link not only thermally but also photonically. A negative pattern is generated after development of a UV-irradiated thin film of hb-P**35** through a copper negative mask (Fig. 15). The hb-PDY synthesized from the triphenylamine-containing monomer emits strong green light when observed under a fluorescence microscope. This is remarkable, considering that many conjugated polymers show weak emissions in the solid state or when fabricated into thin films due to the nonradiative energy transfer

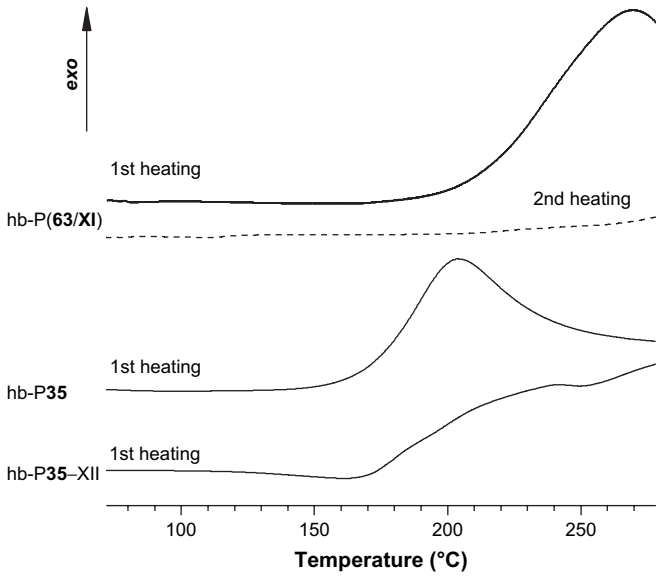

Fig. 14. DSC thermograms of hb-PDYs measured at a scan rate of 10 °C/min under nitrogen.

caused by π–π stacking of the polymer chains or defect formation [82]. Since conventional photoresists such as SU-8 are generally nonluminescent and can thus only be used as a passive material, the bright emission of the hb-PDY may allow it to find applications as active matrix for the fabrications of liquid-crystal displays, light-emitting diodes, and other photonic devices.

Template methods have been widely used to fabricate three-dimensional nano- and microstructured patterns. Breath figure process is a simple way to generate large arrays of patterned assemblies. It has been reported that star-shaped polymers and block copolymers form honeycomb morphologies through an evaporation-induced assembly process [83,84]. Our and other research groups have recently shown that neither star-shaped nor block structure is necessarily needed for the formation of the well-defined assembling morphologies [85–88].

We tried to create assembling structures of hb-PDYs by employing the breath figure process. Fig. 16 shows the photographs of the patterned structures of hb-P**35** formed by blowing a stream of moist air over its CS_2 solutions. Hexagonally ordered hollow bubble arrays with an average void size of ~10 μm are obtained over a large area. Similar to the patterns generated by the UV irradiation through a copper negative mask, the honeycomb patterns obtained from the breath figure process are light-emitting when observed under a fluorescence microscope and can thus potentially be used as the active layers in the fabrication of optical and photonic devices.

7.4. Metal complexation

Acetylene molecules are versatile ligands in organometallic chemistry [16]. For example, acetylene–metal complexes can be formed through covalent interactions of one triple bond with $Co_2(CO)_8$ [89] and two triple bonds with $CpCo(CO)_2$ [90]. The hb-PDYs contain numerous acetylenic triple bonds and can thus be readily metallized through their complexations with the cobalt carbonyls (Scheme 16). Upon admixing hb-P**35** and the cobalt carbonyls in THF at room temperature, the solution color changed from yellow to brown, accompanied by CO gas evolution. The mixtures remained homogenous toward the ends of the reactions and the reaction products were purified by pouring the THF solutions into hexane. The polymer complexes are stable in air, and the incorporation of the cobalt metal is verified by spectral analyses [91].

The as-prepared solution of complex hb-P**65** can be readily spin-coated onto glass or silicon wafer to give a homogenous, yellowish brown-colored thin film. Photoirradiation of the film of the metallized polymer through a copper negative mask causes a decomposition of the cobalt carbonyl complex. The film is readily photobleached, generating a faithful copy of two-dimensional pattern of the photomask without going through any developing processes (Fig. 17). The magnified image shown in Fig. 17B clearly reveals the sharp edges of the photopattern [92,93].

Inspired by the UV light-induced color change of hb-P**65**, we further studied its optical properties in more detail. Similar

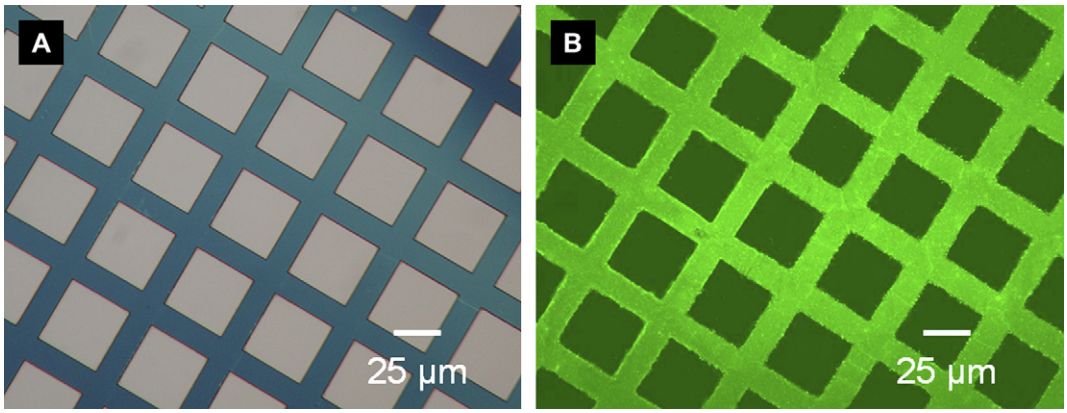

Fig. 15. (A) Optical and (B) fluorescent micrographs of photopatterns generated by photolysis of hb-P**35**.

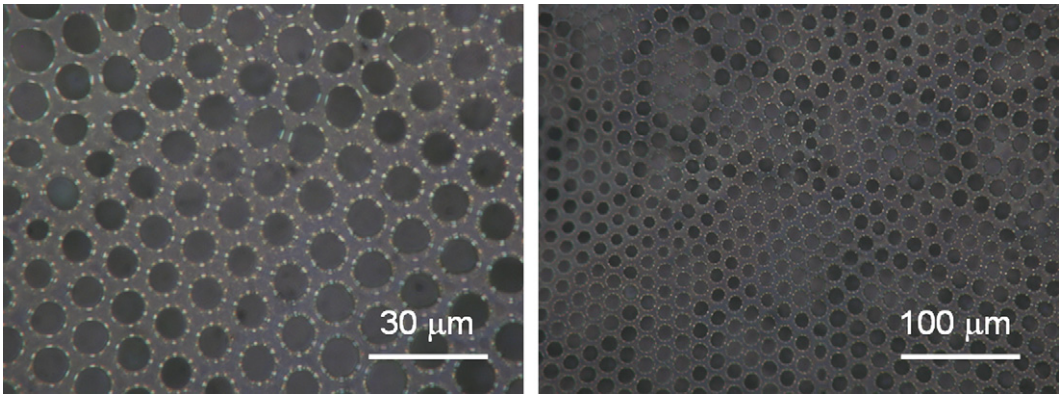

Fig. 16. Optical micrographs of breath figures of hb-P**35** obtained from its CS_2 solutions by blow drying in a stream of moist air.

to its parent of hb-P**35** [80], the metallized polymer exhibits very high refractive index (RI) values ($n = 1.813–1.714$) in the spectral region of 600–1600 nm (Fig. 18) while maintaining a high revised Abbé number ($\upsilon_D' = 60$). Remarkably, the RIs drop significantly after the UV irradiation ($\Delta n = 0.047$). With such a big RI change and a low optical

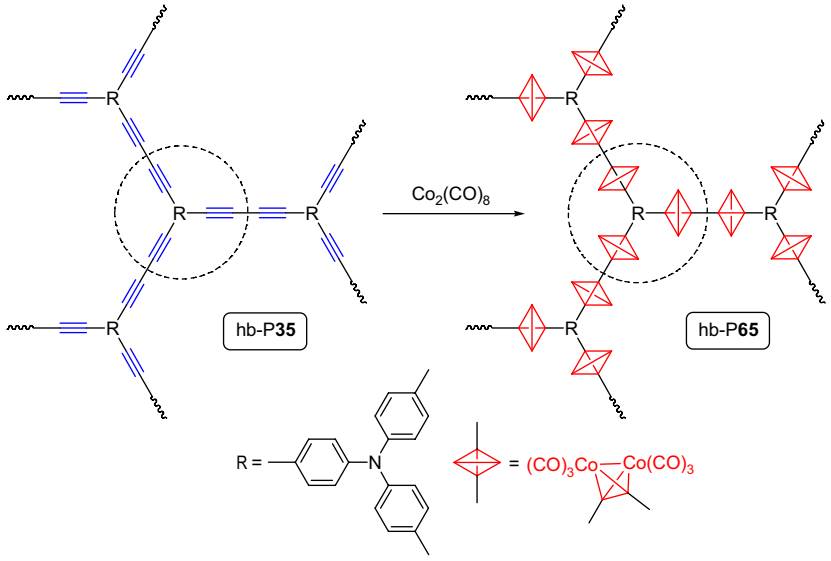

Scheme 16. Preparation of cobalt-containing polymer hb-P**65** via metallization of hb-P**35**.

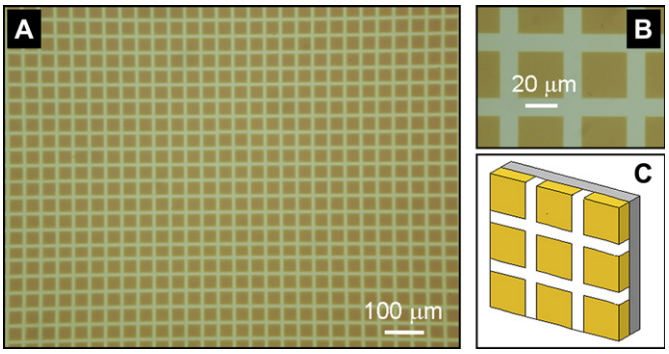

Fig. 17. (A) Optical micrograph of a two-dimensional photonic pattern generated by UV irradiation of hb-P**65** through a Cu-negative mask, (B) image with a high magnification, and (C) model of the photopattern, with brown and white colors denoting unexposed and exposed areas, respectively.

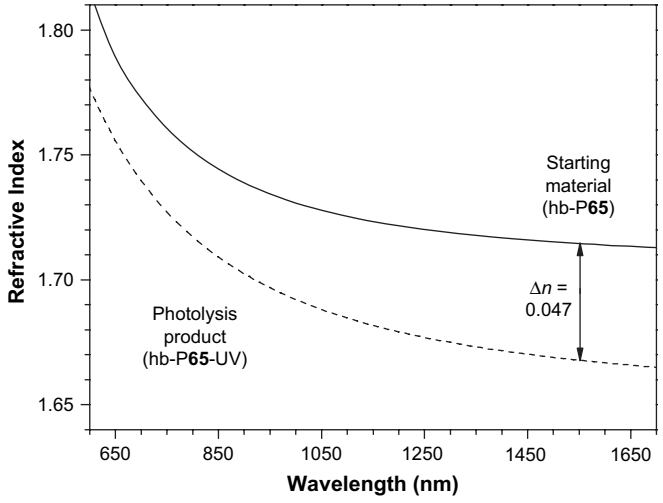

Fig. 18. Refractive indexes of thin films of the cobalt-containing polydiyne before (hb-P**65**) and after photolysis (hb-P**65**-UV).

dispersion, the polymer is promising for an array of photonic applications: it may, for example, serve as photorefractive material in the holographic devices and work as high RI optical coatings.

Metallic species such as iron, nickel and cobalt can catalyze the growth of carbon nanotubes (CNTs) in a chemical vapor deposition (CVD) process. Because of the ready thermal curability of the hb-PDYs, spin-coated films of organometallic polymers hb-P**65** and hb-P**66** are envisioned to hamper the metallic nanoclusters from agglomerating in the CVD process and hence to provide nanoscopic catalyst seeds for the CNT growth. This proves to be the case. As can be seen from Fig. 19, uniform bundles of multi-walled CNTs are grown by the CVD process at 700 °C with acetylene gas as the carbon source. The diameters and lengths of the CNTs are alterable by varying the surface activation and growth time [94]. Thanks to the hyperbranched carbon-rich backbone structure and the thus-achieved depression in the agglomeration of the metallic catalyst seeds, the diameters of the CNTs are small in size (~15 nm) and uniform in size distribution.

7.5. Magnetic ceramization

It has become clear now that the carbon-rich hb-PDYs are readily curable (from ~150 °C), thermally stable (up to ~550 °C), and pyrolytically carbonizable (up to ~80 wt%). Furthermore, their triple bonds are easily metallizable by complexations with cobalt carbonyls. Since the polymer complexes contain a large number of metal atoms, we tried to utilize them as precursors for fabrication of magnetic ceramics. The pyrolyses of the polydiyne–cobalt complexes hb-P**65** and hb-P**66** at 1000 °C for 1 h under nitrogen furnish the ceramic products of C_xCo_y **67** and **68**, respectively, in 50–65% yields (Scheme 17). All the ceramics are magnetizable and can be readily attracted to a bar magnet.

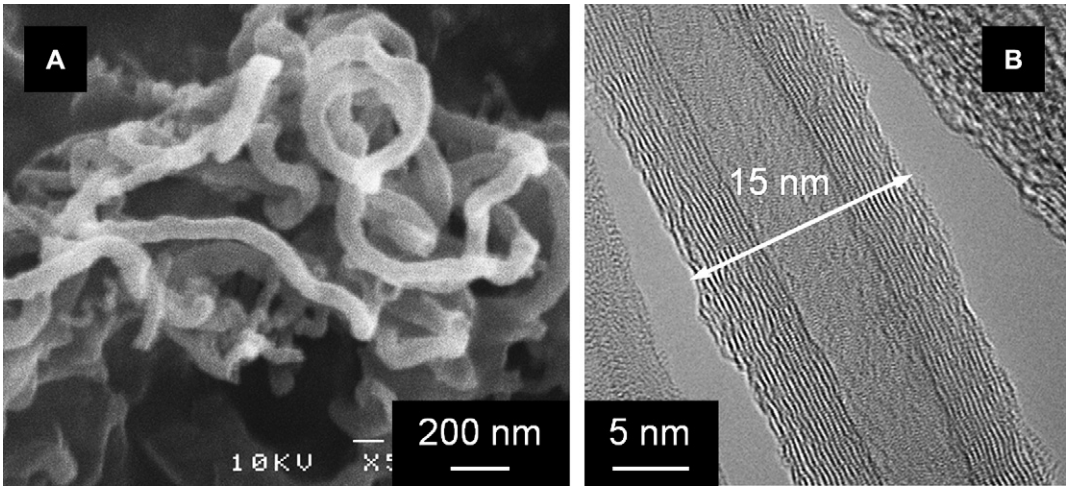

Fig. 19. (A) SEM and (B) TEM microphotographs of the carbon nanotubes prepared by a CVD process at 700 °C on the silicon wafers spin-coated with thin films of hb-P**65**.

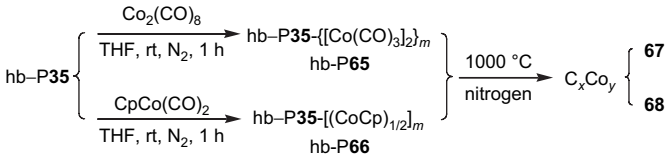

Scheme 17. Complexation of polymer hb-P**35** with cobalt carbonyls and ceramization of the polymer–cobalt complexes hb-P**65** and hb-P**66** to respective magnetic ceramics **67** and **68**.

The magnetization curves of the ceramics at 300 K are shown in Fig. 20. With an increase in the strength of externally applied magnetic field, the magnetization of **67** swiftly increases and eventually levels off at a saturation magnetization (M_s) of ~118 emu/g, which is much higher than that of the magnet used in our daily life ($M_s = 74$ emu/g) [95,96]. The high M_s value of **67**, along with its powder XRD, XPS and SEM data [91], indicates that the cobalt nanocrystallites in the ceramic are well wrapped by carboneous species, which have prevented the cobalt particles from being oxidized during and after the pyrolysis and ceramization processes [96].

Clearly, hb-P**65** is an excellent precursor to magnetoceramics because its three-dimensional spherical cage structure has enabled the retention of the pyrolyzed species and the steady growth of the magnetic crystallites [61,62]. The M_s value of **68** is lower (~26 emu/g), which is understandable, because the cobalt content of its precursor complex (hb-P**66**) is lower. The hysteresis loops of the magnetoceramics are very small. The coercivity (H_c) values of **67** and **68** are 0.058 kOe and 0.142 kOe, respectively. The high magnetizability (M_s up to 118 emu/g) and low coercivity (H_c down to ~0.06 kOe) of **67** make it an outstanding soft ferromagnetic material [96].

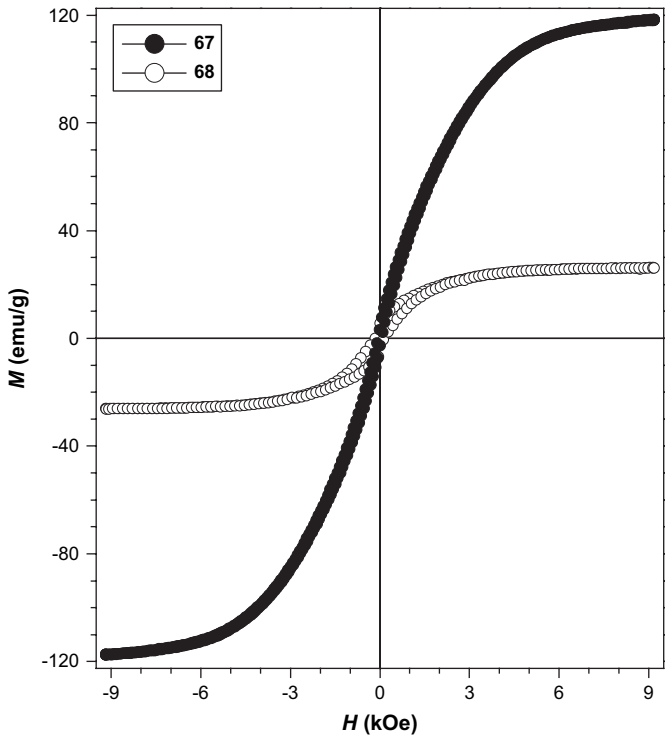

Fig. 20. Plot of magnetization (M) versus applied magnetic field (H) for magnetoceramics **67** and **68**.

8. Conclusion

In this Feature Article we have briefly summarized our efforts and results on the preparations of new hyperbranched polymers, especially on the development of unimolecular A_n systems for the syntheses of a variety of functional polymers from triple-bonded acetylene monomers. Effective polymerization processes including polycyclotrimerization, polycycloaddition and polycoupling of diynes and triynes initiated by metallic and nonmetallic catalysts have been established, which have enabled the creation of hyperbranched polyphenylenes, polytriazoles and polydiynes with high molecular weights and excellent macroscopic processability in high yields. The new polymerization routes opened and the new structural insights gained in this study offer versatile synthetic tools and valuable design guidelines for the further developments in the area of research.

Using the triple-bond building blocks in combination with the functional groups has resulted in the creation of hyperbranched π-conjugated polymers with advanced materials properties. The carbon-rich polymers showed outstanding thermal stability. Incorporation of luminophoric units into the structures of the polymers enabled the modulation of their emission colors and efficiencies at the molecular level. The numerous aromatic rings in the hb-PArPs conferred strong optical limiting power on the polymers, while the poled thin films of the azo-functionalized hb-PAEs showed stable NLO performance with high SHG coefficients. Combination of the slim diyne linker with the polarizable triphenylamine core brought about excellent optical transparency and exceptionally high photorefractivity. The photonically susceptible benzyl, benzophenone and diyne units endowed the polymers with high photocurability and hence the potential to be used as sensitive photoresists and active matrixes in the construction of optical devices. The assemblies of the hexagonal arrays of the breath figures and the micrometer-long polymer nanotubes were obtained from the dynamic and static templating processes. The complexations with the cobalt carbonyls yield spin-coatable hyperbranched organometallic polymers, whose RIs were readily tuned by UV irradiation to a very large extent. The hyperbranched polymer–cobalt complexes served as excellent precursors to soft ferromagnetic ceramics and as nanosized catalyst seeds for the fabrication of CNTs.

The simple synthesis and ready processability of the hyperbranched polymers, coupled with their unique molecular structures and useful functional properties, make them attractive and promising for an array of high-technology applications. Further studies on the syntheses, properties and applications of new acetylene-based hyperbranched polymers are under way in our laboratories.

Acknowledgement

The work described in this Feature Article was partially supported by the Research Grants Council of Hong Kong (602706, HKU2/05C, 603505, and 603304), the National Science Foundation of China (20634020), and the Ministry of Science and Technology of China (2002CB613401). We thank all the people involved in this project, some of whose names can be found in the references given below. B. Z. T. thanks the support from the Cao Guangbiao Foundation of Zhejiang University.

References

[1] Shirakawa H. Angew Chem Int Ed 2001;40:2575.
[2] MacDiarmid AG. Angew Chem Int Ed 2001;40:2581.
[3] Heeger AJ. Angew Chem Int Ed 2001;40:2591.
[4] Masuda T, Higashimura T. Acc Chem Res 1984;17:51.
[5] Masuda T, Higashimura T. Adv Polym Sci 1986;81:121.
[6] Diederich F, Gobbi L. Top Curr Chem 1999;201:43.
[7] Watson MD, Fechtenkotter A, Mullen K. Chem Rev 2001;101:1267.
[8] Yashima E. Anal Sci 2002;18:3.
[9] Mayershofer MG, Nuyken O. J Polym Sci Part A Polym Chem 2005; 43:5723.
[10] Ray CR, Moore JS. Adv Polym Sci 2005;177:91.
[11] Bunz UHF. Adv Polym Sci 2005;177:1.
[12] Aoki T, Kaneko T, Teraguchi M. Polymer 2006;47:4867.
[13] Masuda T. J Polym Sci Part A Polym Chem 2007;45:165.
[14] Akagi K. Bull Chem Soc Jpn 2007;80:649.
[15] Shirakawa H, Masuda T, Takeda T. In: Patai S, editor. The chemistry of triple-bonded functional groups. Chichester: Wiley; 1994.
[16] Stang PJ, Diederich F, editors. Modern acetylene chemistry. Weinheim: VCH; 1995.
[17] Patai S, editor. The chemistry of the carbon–carbon triple bond. New York: Wiley; 1978.
[18] Lam JWY, Tang BZ. Acc Chem Res 2005;38:745.
[19] Lam JWY, Tang BZ. J Polym Sci Part A Polym Chem 2003;41:2607.
[20] Kim YH. J Polym Sci Part A Polym Chem 1998;36:1685.
[21] Hult A, Johansson M, Malmström E. Adv Polym Sci 1999;143:1.
[22] Hawker CJ. Curr Opin Colloid Interface Sci 1999;4:117.
[23] Inoue K. Prog Polym Sci 2000;25:453.
[24] Voit BI. J Polym Sci Part A Polym Chem 2000;38:2505.
[25] Grayson SM, Frechet JMJ. Chem Rev 2001;101:3819.
[26] Tomalia DT, Frechet JMJ. J Polym Sci Part A Polym Chem 2002; 40:2719.
[27] Xu K, Tang BZ. Chin J Polym Sci 1999;17:397.
[28] Lam JWY, Luo J, Peng H, Xie Z, Xu K, Dong Y, et al. Chin J Polym Sci 2000;19:585.
[29] Xu K, Peng H, Sun Q, Dong Y, Salhi F, Luo J, et al. Macromolecules 2002;35:5821.
[30] Zheng RH, Dong HC, Peng H, Lam JWY, Tang BZ. Macromolecules 2004;37:5196.
[31] Li Z, Lam JWY, Dong YQ, Dong YP, Sung HHY, Williams ID, et al. Macromolecules 2006;39:6458.
[32] Grayson SM, Frechet JMJ. Macromolecules 2001;34:6542.
[33] Peng H, Cheng L, Luo JD, Xu KT, Sun QH, Dong YP, et al. Macromolecules 2002;35:5349.
[34] Xie Z, Lam JWY, Dong Y, Qiu C, Kwok HS, Tang BZ. Opt Mater 2002;21:231.
[35] Peng H, Luo J, Cheng L, Lam JWY, Xu K, Dong Y, et al. Opt Mater 2002;21:315.
[36] Xie ZL, Peng H, Lam JWY, Tang BZ. Macromol Symp 2003;195:179.
[37] Lam JWY, Chen JW, Law CCW, Tang BZ. Macromol Symp 2003;196:289.
[38] Häußler M, Lam JWY, Zheng R, Peng H, Luo J, Chen J, et al. C R Chim 2003;6:833.
[39] Dong H, Lam JWY, Häußler M, Zheng R, Peng H, Law CCW, et al. Curr Trend Polym Sci 2004;9:15.
[40] Chen J, Peng H, Law CCW, Dong YP, Lam JWY, Williams ID, et al. Macromolecules 2003;36:4319.
[41] Law CCW, Chen JW, Lam JWY, Peng H, Tang BZ. J Inorg Organomet Polym 2004;14(1):39.
[42] Häußler M, Dong H, Lam JWY, Zheng R, Qin A, Tang BZ. Chin J Polym Sci 2005;23:567.
[43] Häußler M, Tang BZ. Adv Polym Sci 2007;209:1.
[44] Häussler M, Liu J, Zheng R, Lam JWY, Qin A, Tang BZ. Macromolecules 2007;40:1914.
[45] Shi J, Tong B, Zhao W, Shen J, Zhi J, Dong YP, et al. Macromolecules 2007;40:5612.
[46] Kong X, Lam JWY, Tang BZ. Macromolecules 1999;32:1722.
[47] Zheng R, Dong H, Tang BZ. In: Abd-El-Azi A, Carraher C, Pittman C, Sheats J, Zeldin M, editors. Macromolecules containing metal- and metal-like elements, vol. 4. New York: Wiley; 2005. p. 7.
[48] Zheng R, Häussler M, Dong H, Lam JWY, Tang BZ. Macromolecules 2006;39:7973.
[49] Häußler M, Liu J, Lam JWY, Qin A, Zheng R, Tang BZ. J Polym Sci Part A Polym Chem 2007;45:4249.
[50] Luo J, Xie Z, Lam JWY, Cheng L, Chen H, Qiu C, et al. Chem Commun 2001;1740.
[51] Chen J, Law CCW, Lam JWY, Dong YP, Lo SMF, Williams ID, et al. Chem Mater 2003;15:1535.
[52] Chen J, Xie Z, Lam JWY, Law CCW, Tang BZ. Macromolecules 2003;36:1108.
[53] Tutt LW, Kost A. Nature 1992;356:225.
[54] Tang BZ, Leung SM, Peng H, Yu NT, Su KC. Macromolecules 1997; 30:2848.
[55] Balasubramanian K, Selvaraj S, Venkataramani PS. Synthesis 1980;29.
[56] Dong H, Zheng R, Lam JWY, Häussler M, Tang BZ. Macromolecules 2005;38:6382.
[57] Tang BZ, Jim CKW, Qin A, Haeussler M, Lam JWY. US Patent Appln No. US60/933,884; 2007.
[58] Jikei M, Kakimoto M. Prog Polym Sci 2001;26:1233.
[59] Hasegawa M, Horie K. Prog Polym Sci 2001;26:259.
[60] Kim KH, Jang S, Harris FW. Macromolecules 2001;34:8925.
[61] Sun Q, Xu K, Peng H, Zheng R, Häussler M, Tang BZ. Macromolecules 2003;36:2309.
[62] Sun Q, Lam JWY, Xu K, Xu H, Cha JAK, Zhang X, et al. Chem Mater 2000;12:2617.
[63] Häußler M, Sun Q, Xu K, Lam JWY, Dong H, Tang BZ. J Inorg Organomet Polym 2005;15:67.
[64] Rostovtsev VV, Green LG, Fokin VV, Sharpless KB. Angew Chem Int Ed 2002;41:2596.
[65] Scheel AJ, Komber H, Voit BI. Macromol Rapid Commun 2004;25: 1175.
[66] Qin A, Haeussler M, Lam JWY, Tse KKC, Tang BZ. Polym Prepr 2006;47(2):681.
[67] van Steenis DJVC, David ORP, van Strijdonck GPF, van Maarseveen JH, Reek JNH. Chem Commun 2005;4333.
[68] Bakbak S, Leech PJ, Carson BE, Saxena S, King WP, Bunz UHF. Macromolecules 2006;39:6793.
[69] Qin A, Jim CKW, Lu W, Lam JWY, Häuβler M, Dong Y, et al. Macromolecules 2007;40:2308.
[70] Chan TR, Hilgraf R, Sharpless KB, Fokin VV. Org Lett 2004;6:2853.
[71] Bunz UHF. Acc Chem Res 2001;34:998.
[72] Negishi EI, Anastasia L. Chem Rev 2003;103:1979.
[73] Bharathi P, Moore JS. Macromolecules 2000;33:3212.
[74] Kim C, Chang Y, Kim JS. Macromolecules 1996;29:6353.
[75] Weder C. Chem Commun 2005;5378.
[76] Dong YQ, Li Z, Lam JWY, Dong YP, Feng XD, Tang BZ. Chin J Polym Sci 2005;23:665.
[77] Li Z, Qin A, Lam JWY, Dong YQ, Dong YP, Ye C, et al. Macromolecules 2006;39:1436.
[78] Burland DM, Miller RD, Walsh CA. Chem Rev 1994;94:31.
[79] Hay AS. J Polym Sci Part A Polym Chem 1998;36:505.

[80] Häussler M, Zheng RH, Lam JWY, Tong H, Dong HC, Tang BZ. J Phys Chem B 2004;108:10645.
[81] Hergenrother PM. In: Kroschwitz JI, editor. Concise encyclopedia of polymer science and engineering. New York: Wiley; 1990. p. 5.
[82] Hua JL, Lam JWY, Dong H, Wu L, Wong KS, Tang BZ. Polymer 2006;47:18.
[83] Widawski G, Rawiso M, Francois B. Nature 1994;369:387.
[84] Jenekhe SA, Chen XL. Science 1999;283:372.
[85] Tang BZ. Polym News 2001;26:262.
[86] Salhi F, Cheuk KKL, Sun Q, Lam JWY, Cha JAK, Li G, et al. J Nanosci Nanotechnol 2001;1:137.
[87] Srinivasarao M, Collings D, Philips A, Patel S. Science 2001;292:79.
[88] Peng J, Han Y, Li B. Polymer 2004;45:447.
[89] Newkome GR, He EF, Moorefield CN. Chem Rev 1999;99:1689.
[90] Nishihara H, Kurashina M, Murata M. Macromol Symp 2003;196:27.
[91] Häußler M, Lam JWY, Zheng R, Dong H, Tong H, Tang BZ. J Inorg Organomet Polym Mat 2005;15:519.
[92] Häußler M, Lam JWY, Qin A, Tse KKC, Li MKS, Liu J, et al. Chem Commun 2007;2584.
[93] Wilson J. Chem Technol 2007;4:T42.
[94] Häußler M, Tse KC, Lam JWY, Tong H, Qin A, Tang BZ. Polym Mater Sci Eng 2006;95:213.
[95] Tang BZ, Geng Y, Lam JWY, Li B, Jing X, Wang X, et al. Chem Mater 1999;11:1581.
[96] O'Handley RC. Modern magnetic materials: principles and applications. New York: Wiley; 2000. p. 491.

Matthias Häußler received his Master degree in Chemistry from Martin-Luther University Halle-Wittenberg, Germany in 2002. He then joined Prof. B. Z. Tang's group at The Hong Kong University of Science & Technology (HKUST), where he carried out his Ph.D. study on hyperbranched π-conjugated polymers. After the successful completion of his Ph.D. study in summer 2006, he accepted an OCE Fellowship from the Commonwealth Scientific and Industrial Research Organization in Melbourne, Australia, where he is now working on the development of new organic photovoltaic and electroactive materials.

Anjun Qin received his Ph.D. degree in Physical Chemistry and Materials Science from Institute of Chemistry of Chinese Academy of Science in 2004 under the supervisions of Profs. C. Ye and F. Bai. From 2005 to 2006, he worked as a postdoctoral associate in Prof. B. Z. Tang's group at HKUST. From the beginning of 2007, he started his postdoctoral work in the Department of Polymer Science and Technology at Zhejiang University. He has been working on the construction of functional linear and hyperbranched polymers from acetylenic triple-bond building blocks, especially on the exploration of efficient catalyst systems and new polymerization reactions.

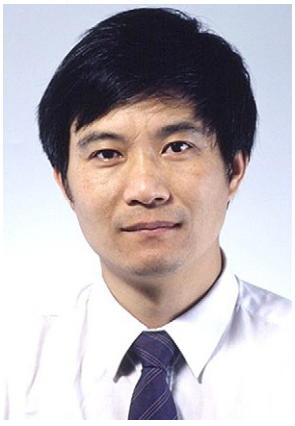

Ben Zhong Tang carried out his Ph.D. study in Polymer Chemistry under the supervisions of Profs. T. Higashimura and T. Masuda at Kyoto University, Japan. He worked as a senior research scientist in the Central Laboratory of Neos Corp., Japan, and conducted his postdoctoral research under the supervision of Prof. I. Manners at University of Toronto, Canada. In July 1994, he joined the Department of Chemistry of HKUST. He is now a professor of chemistry at HKUST and the Cao Guangbiao Chair Professor at Zhejiang University. He is currently on the editorial boards of *Progress in Polymer Science*, *Macromolecular Chemistry and Physics*, *Journal of Nanoscience and Nanotechnology*, *Journal of Inorganic and Organometallic Polymers*, *Journal of Polymer Materials*, and *Acta Polymerica Sinica*. He received the Croucher Senior Research Fellowship Award from Croucher Foundation and the Wang Baoren Award for Accomplishments in Fundamental Polymer Research from Chinese Chemical Society, both in 2007 and the Distinguished Young Scholar Award (for scientific researchers of Chinese origin) from National Science Foundation of China in 2002.